N69-35443

TRACKING AND DATA ACQUISITION FOR SPACE EXPLORATION

Robert J. Coates

Goddard Space Flight Center
Greenbelt, Maryland

May 1969

YOUR KEY...

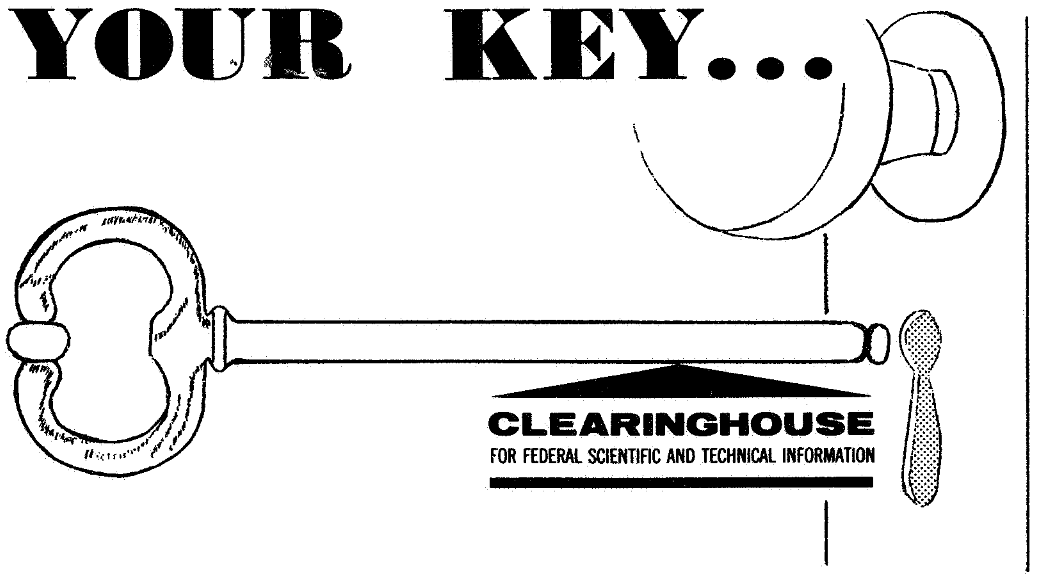

to scientific and technical advancement

Mr. Scientist. . .Engineer. . .Businessman. . .the Clearinghouse for Scientific and Technical Information can serve as your key to progress in research and development. Each year, some 40,000 unclassified documents from more than 125 Government agencies enter our collection. The Clearinghouse announces, reproduces and sells these reports to the public at a nominal cost. To make this wealth of scientific and technical information readily available, we have tailored our services to meet the needs of the highly selective customer as well as the general user. Some of these services are listed below.

U.S. GOVERNMENT RESEARCH AND DEVELOPMENT REPORTS (USGRDR). This semimonthly journal abstracts approximately 40,000 new Government-sponsored reports and translations annually. Features a quick-scan format, cross references, edge index to subject fields, and a report locator list.

U. S. GOVERNMENT RESEARCH AND DEVELOPMENT REPORTS INDEX (USGRDR-I). Published concurrently with the USGRDR to index each issue by subject, personal author, corporate source, contract number and accession/report number. Quarterly Indexes and an Annual Cumulative also are available.

CLEARINGHOUSE ANNOUNCEMENTS IN SCIENCE AND TECHNOLOGY. A semimonthly current awareness announcement service in 46 separate categories representing complete coverage of all documents announced by the Clearinghouse. Highlights special interest reports.

FAST ANNOUNCEMENT SERVICE (FAS). Selective announcement service emphasizing commercial applications of report information. Covers approximately 10 percent of Clearinghouse document input. Compiled and mailed in 57 categories.

SELECTIVE DISSEMINATION OF MICROFICHE (SDM). Automatic distribution twice monthly of Government research and development reports on microfiche. Economical and highly selective. Several hundred categories from which to choose.

ADDITIONAL INFORMATION concerning these and other Clearinghouse services is available by writing to:

Customer Services
Clearinghouse
U.S. Department of Commerce
Springfield, Virginia 22151

☆ U. S. GOVERNMENT PRINTING OFFICE : 1969 O - 360-245

2P

X-520-69-200

PREPRINT

NASA TM X- 63629

TRACKING AND DATA ACQUISITION FOR SPACE EXPLORATION

ROBERT J. COATES

MAY 1969

GSFC
GODDARD SPACE FLIGHT CENTER
GREENBELT, MARYLAND

FACILITY FORM 602
N69-35443 (ACCESSION NUMBER)
75 (PAGES)
NASA-TMX-#63629 (NASA CR OR TMX OR AD NUMBER)
1 (THRU)
(CODE)
30 (CATEGORY)

X-520-69-200

TRACKING AND DATA ACQUISITION FOR SPACE EXPLORATION

Robert J. Coates

May 1969

GODDARD SPACE FLIGHT CENTER
Greenbelt, Maryland

TRACKING AND DATA ACQUISITION FOR SPACE EXPLORATION*

Robert J. Coates

ABSTRACT

The tracking and data acquisition systems provide the key link between the remote spacecraft and the scientific experimenter on the ground. The operation of the space experiment takes place through the links of command, telemetry and tracking. The evolution from the early very simple spacecraft missions toward more complex and sophisticated missions has been paralleled by a similar evolution in the tracking and data acquisition systems. The early Minitrack interferometer tracking system still carries the major tracking workload for space missions; however greater tracking accuracy requirements for more recent missions, such as the Orbiting Geophysical Observatory and the Apollo mission, have brought about the development of unified tracking and data acquisition systems which utilize hybrid pseudo-random code/sidetone ranging techniques. The data acquisition has evolved from analog telemetry systems to the present day heavy use of PCM digital telemetry. Likewise the command systems have evolved from early simple 'on/off' command systems into PCM digital command data systems. The trend is toward greater real time control of more complex functions on board the spacecraft. Newer spacecraft are incorporating computer-type systems in the spacecraft which require programming and memory load through the ground command link. The most attractive concept for the next generation network for tracking and data acquisition is a network consisting of synchronous-orbit Tracking and Data Relay Satellites for covering launches and low-orbit earth satellites plus a few selected stations for supporting spacecraft in high earth orbit and lunar orbit.

*Space Science Reviews 9 (1969) 361-418.

CONTENTS

1. *INTRODUCTION*

The design of flight missions for space exploration always must take into consideration the design and capability of the tracking and data acquisition systems because they provide the key link between the remote automated spacecraft and the scientific experimenter on the ground. The complete operation of the experiment must take place through the links of command, telemetry and tracking. The achievement of the scientific objectives of many missions are determined by the capabilities of these ground systems. For example, the determinations of geodetic quantities with artificial satellites are limited by the capability to track and determine precise orbits of the geodetic satellites. Often the amount of data that can be acquired in a particular experiment is restricted by the maximum bit rate capability of the telemetry link. Likewise the control of extremely complex spacecraft may be limited by the command systems characteristics. Thus, the design of the tracking, command, and data acquisition capability is a very important consideration.

At first glance one might assume that a flight mission would be able to design their unique tracking and data acquisition network to the optimum for their particular flight mission. However, this is not the case because of economic considerations. The support of even a single flight mission would require the establishment of numerous stations located at remote sites all over the world. It would be much more economical to design a worldwide tracking and data acquisition network that would have the capability of supporting many flight missions. Thus the total job could be done much more economically. At the present time, most of the tracking and data acquisition networks for support of scientific space exploration are configured for providing multimission support. The configuration of the particular space network is determined largely by the unique characteristics of the particular group of missions which are to be supported. For example, the United States National Aeronautics and Space Administration has three tracking and data acquisition networks for supporting space exploration. The Space Tracking and Data Acquisition Network (STADAN) is designed to handle automated unmanned satellites in earth orbits with either high or low inclinations and with various orbit heights ranging from the minimum altitudes up to lunar distances. The Manned Space Flight Network is designed specifically to support the manned space explorations. The NASA Deep Space Network provides tracking and data acquisition support to lunar, planetary, and deep space missions. This paper will discuss many of the factors which are important in the design of a multi-mission tracking and data acquisition network for space exploration.

2. TRACKING

Tracking is required for each orbiting spacecraft in order to determine the location of the spacecraft at the time of each scientific measurement. In addition, tracking must provide pointing information to the ground stations so that data acquisition antennas can be pointed at the spacecraft to receive the spacecraft telemetry signals. All tracking systems for locating orbiting scientific spacecraft measure one or more of the quantities of angular position, angular velocity, range, and range-rate of the spacecraft.

Since most spacecraft collect data continuously, the complete time history of spacecraft position and velocity must be determined. Sophisticated theories of orbit mechanics enable the calculation of the spacecraft orbits from a relatively small amount of tracking data. Thus most space tracking networks consist of a few stations located around the world at sites selected to provide a sufficient number and spacing of tracking measurements to enable accurate calculation of the orbits.

There are several criteria which must be followed in the selection of locations for the stations in a tracking network. The first requirement is for very early tracking data immediately after launch in order to determine if the launch was successful and orbit has been achieved. Next there should be some tracking of the spacecraft at least once per orbit as a minimum. In order to determine accurate orbits it is necessary to have tracking from opposite sides of the orbit. In addition to these minimum requirements, it is mandatory to cover any thrusting maneuvers with accurate tracking in order to determine the change in orbit due to the thrusting. A further determining factor in the location of tracking stations are the other requirements for data acquisition and command, because generally all three functions are performed by the same ground stations. As will be seen later, in many of the optimum systems for tracking, the tracking, command and data acquisition functions are combined into the same system.

The locations of the Minitrack tracking systems in STADAN illustrate the application of the criteria to the design of a tracking network. The first worldwide tracking network for orbiting spacecraft was the Minitrack Network which used the *Minitrack tracking system* (Mengel and Herget, 1958; Schroeder, 1960). It was conceived for the United States Vanguard Satellite Program, and it continues to be the tracking system most heavily used by scientific spacecraft launched from the United States. The present STADAN contains many of the original Minitrack Network stations. The locations of the Minitrack tracking systems in STADAN are shown in Figure 1. There are 10 Minitrack sites. The network supports both low inclination satellites launched from Cape Kennedy, Florida, and high inclination satellites launched from the Western Test Range, California. The Minitrack sites at Johannesburg, South Africa, and Tananarive,

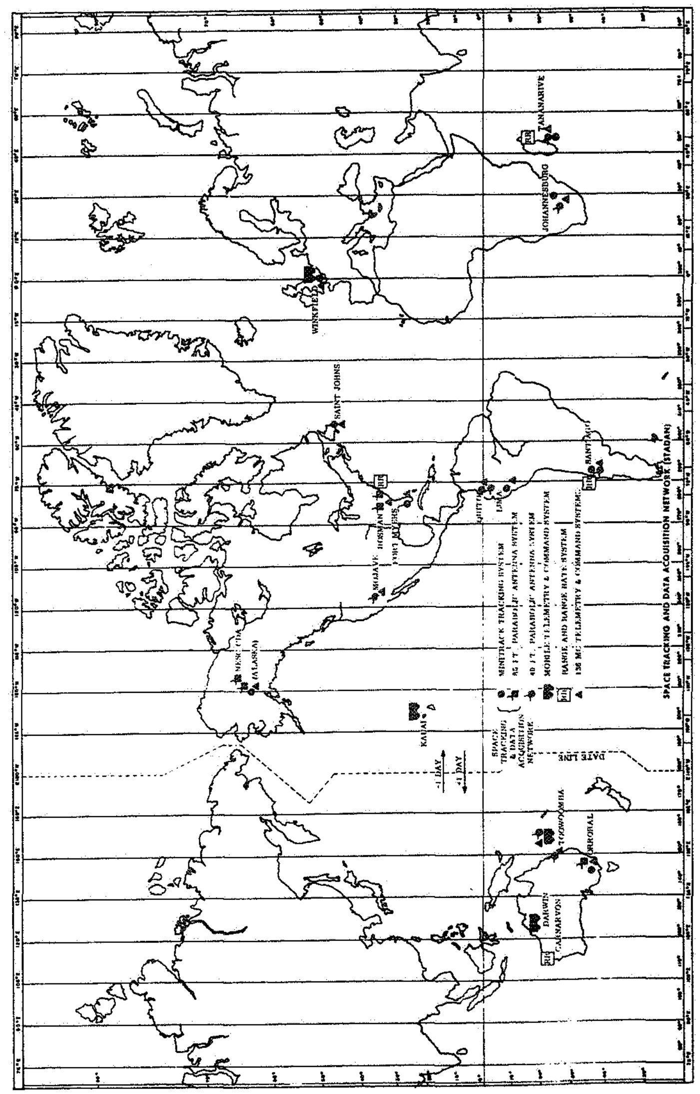

Figure 1. NASA Space Tracking and Data Acquisition Network (STADAN) station locations.

Madagascar, provide tracking early in the first orbit soon after launch from either Florida or California. The stations at St. John's, Newfoundland; Fort Myers, Florida; Quito, Ecuador; Lima, Peru; and Santiago, Chile make up a North-South 'fence' which contacts a low inclination orbit satellite once an orbit. The addition of the sites at Fairbanks, Alaska and Winkfield, England create an East-West 'fence' for contacting polar orbiting satellites at least once an orbit. The station at Orroral, Australia provides post-launch tracking for Northeast launches from Cape Kennedy, Florida. But primarily Orroral provides very frequent tracking on the opposite side of the orbit from the tracking obtained with the North-South 'fence'. These Minitrack locations provide sufficient data for moderately accurate orbit determination from the first three orbits of a satellite mission. This has proven to be quite adequate for most unmanned scientific space missions.

A. Minitrack Interferometer Tracking System

The Minitrack system was so named because minimum weight was required aboard the spacecraft for tracking. It was the first of many unified tracking and telemetry systems that are utilized in space exploration because of the large savings in weight and power. The Minitrack system is an angle measuring interferometer system which measures the angle of arrival of the radio signal transmitted from the spacecraft. In most spacecraft systems, the carrier of the telemetry transmitter provides the Minitrack signal. The Minitrack system for determining satellite positions is based on the interferometer principle. When two antennas separated by a fixed distance of $N\lambda$ (N = constant and λ = wavelength) receive radiation from a distant source (such as a satellite) at an angle θ with the baseline of the two antennas, the received signals at the two antenna terminals differ in phase by $\Delta\phi = 2\pi N \cos\theta$ radians. Thus, by measuring this difference in phase, one can determine the angle θ from the above relation. Two sets of interferometers, one with an East-West baseline and one with a North-South baseline, are used to measure the two direction cosines for specifying a satellite position. The antenna field for the Minitrack system (G.S.F.C., 1964) is shown in Figure 2. The Minitrack system uses two different sets of East-West and North-South long baseline interferometers. The reason for this is that the Minitrack antennas are eight-element slot arrays which have a fan shaped beam of approximately 76° by 11° at the 3 db point. The four antennas marked 'equatorial' have the fan beam oriented North-South for low inclination orbits, and the second set of antennas marked 'polar' have the beam oriented East-West for tracking satellites in high inclination orbits. The equatorial or polar tracking modes are selectable by switching to the desired sets of antennas. The two pairs of antennas having baselines of approximately 57 wavelengths (or 46 wavelengths) obtain the highest angular resolution. These are termed 'fine' antennas. Because the phase meters repeat their reading cycle every wavelength of path difference, an ambiguity results. This is resolved by employing several

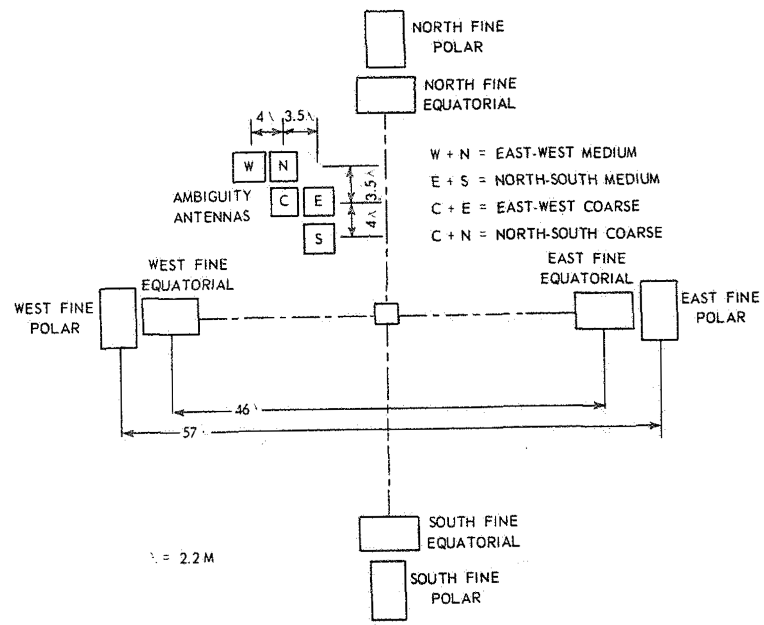

Figure 2. Minitrack antenna field.

progressively shorter baselines which produce fewer integral numbers of wavelength changes while the satellite is within the antenna pattern.

The ambiguity antennas have a beamwidth of 78° by 106°. This allows the use of one set of ambiguity interferometers for both high- and low-inclination orbits. The ambiguity antennas form a North-South 'medium' interferometer, an East-West 'medium' interferomter, a North-South 'course' interferometer, and an East-West 'course' interferometer. The baselines of the 'medium' and 'course' interferometers are 4.0 and 3.5 wavelengths respectively. The reason for selecting this arrangement is that the physical size of the antennas makes it impractical to obtain directly a half-wavelength baseline. An equivalent 0.5 wavelength baseline is obtained by subtracting the phase of the 3.5 wavelength baseline from the phase of the 4.0 wavelength baseline. Also an equivalent 7.5 wavelength baseline is obtained by adding the two phase values. The 0.5 baseline phase is used to resolve the ambiguity of the 4.0 wavelength baseline phase which in turn resolves the ambiguity of the 7.5 wavelength baseline phase. Ambiguity antenna information identifies the integral number of wavelengths of path difference on the fine antenna. Data from the fine antenna baseline determines the direction cosines of the satellite which are the basis for the orbital calculations.

Each antenna pair feeds a channel in the receiver, yielding six separate phase measurements. The Minitrack receiver is a 7-channel, triple conversion superheterodyne, tunable over the 136-137 MHz in 1-kHz steps. Six channels carry satellite tracking information, and one channel is reserved for system calibration. The diagram of the Minitrack receiving system is shown in Figure 3. The Minitrack receiver differs from ordinary receivers in that it uses two separate front-end chassis, each containing a low noise r.f. amplifier and a mixer. The receiver uses two first local oscillator signals which are separated in frequency by 100 Hz. This 100-Hz separation is phase-locked to a 100-Hz frequency standard. Each antenna of the 136-MHz interferometer system is connected to a separate front-end chassis. These chassis have several inputs to permit each antenna channel to be used in several phase measuring combinations. The signal from one of a pair of antennas is amplified in the front end unit and is then translated in the mixer to the first i.f. frequency. The signal from the second antenna of the pair is amplified in the other front end unit and converted with the local oscillator whose frequency differs from that of the first oscillator by 100 Hz. The two front-end output signals, which are separated in frequency by the 100-Hz difference in their respective local oscillators, are combined and fed into the first i.f. amplifier. Only the minimum gain necessary for good noise figure is used prior to the combining of the two signals in order to reduce the drift in differential phase between the two signals. After combining, both signals travel through the same i.f. amplifiers and mixers in order to greatly reduce the possibility of appreciable differential phase shifts. Most of the amplification in the receiver is in the first, second, and third i.f. amplifiers. A detector following the third i.f. amplifier mixes the combined signals. The resultant 100-Hz difference frequency is passed through a 100-Hz filter (2-Hz bandwidth for ambiguity channels and 10-Hz bandwidth for fine channels) in order to reduce excess noise. The two first local oscillator frequencies are mixed together and their 100-Hz difference frequency is taken out for a reference signal. The relative phase between the 100-Hz reference and the 100-Hz receiver output is, except for fixed shifts, the same as the relative phase between the r.f. signals received at the two antennas. The phase of each receiver output relative to the reference signal is measured with a phase meter and recorded for a record of the r.f. phase between the two antenna signals. Precise resolution of the fine interferometer data is furnished by a digital phase meter. East-West and North-South fine data are read digitally five times per second. Data readout time is synchronized with clock time which has an accuracy of ±1 millisec.

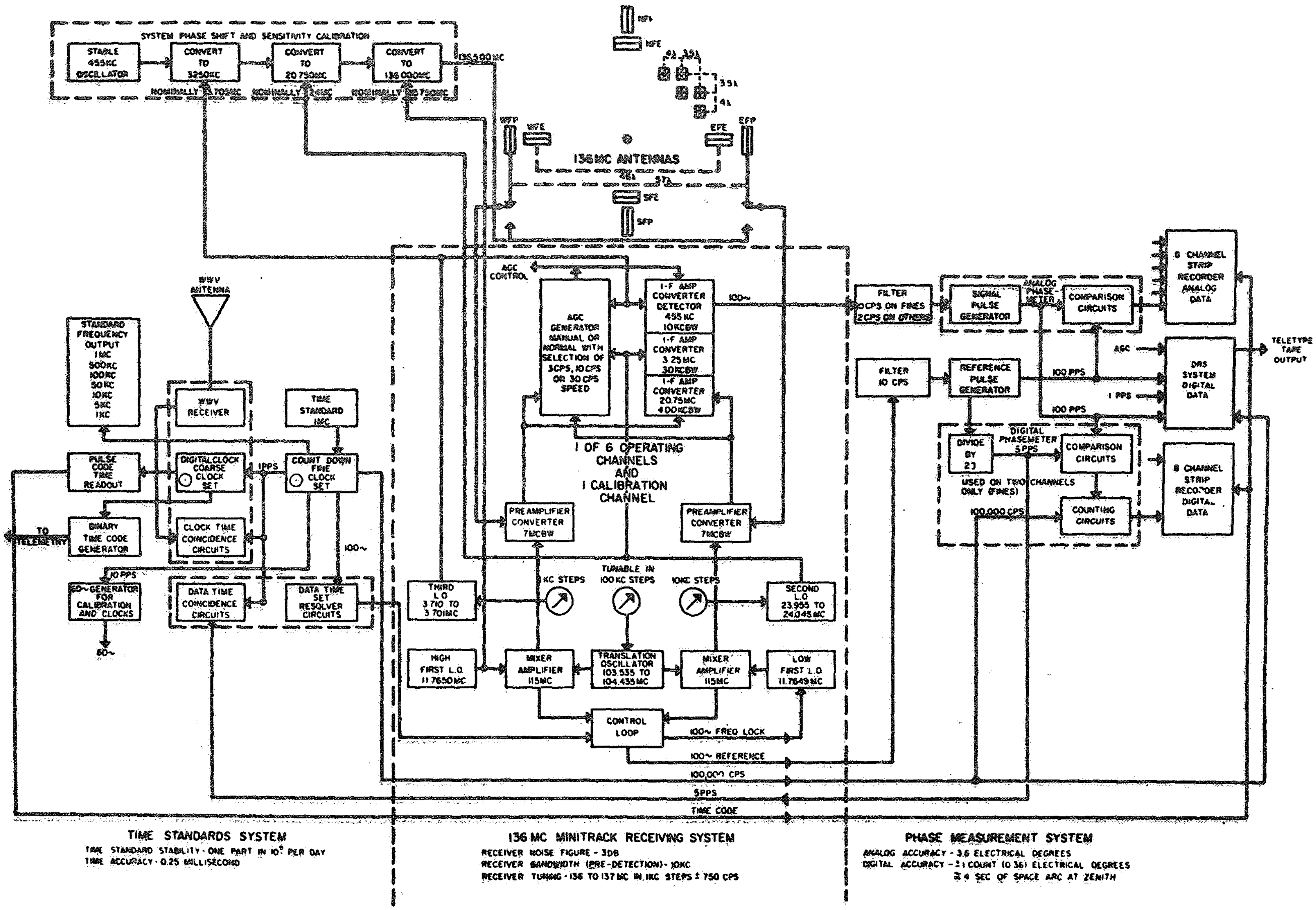

Figure 3. Minitrack interferometer system block diagram.

In addition to the Minitrack antenna system, a 40-inch focal length camera is located at the exact center of the fine beam arrays of the antenna system. This camera is used for calibrating the antenna system by photographing an airborne flashing light beacon against the background of stars while the antenna system is simultaneously receiving a 136-MHz radio signal from the same airborne source.

The digital phase meter used in the Minitrack system provides a resolution in space angle of about 4 sec of arc. The aircraft calibration of each Minitrack station is necessary to determine the distortions of the antenna field, electronic biases, and the general operating health of the system. The biases and distortions are the determining factors in the overall accuracy of the system. Recent comparisons of simultaneous tracking of the GEOS 1 spacecraft by Minitrack and other radio and optical tracking systems (Marsh et al., 1967) have demonstrated that orbits computed from Minitrack data alone have residuals of only 0.2 milliradians. An angular error of 0.2 milliradians for a 500 km spacecraft height is approximately equivalent to a positional error of 100 m.

B. Range and Range Rate Tracking

An angle tracking system, such as Minitrack, is optimum for approximately circular orbits of moderate to low height. There are a number of other orbits for which the range and range rate type of tracking system is more optimum for tracking. For example, the highly eccentric orbit of the OGO satellite has an apogee of 120000 km. An angular error of 0.2 milliradians at apogee would correspond to a positional error of the order of 24 km. As another example, a ranging system is more optimum for determining synchronous altitude orbits. A ranging system is also required for extremely precise orbit determination where the position of the satellite must be determined to an accuracy of considerably less than 100 m.

Radio ranging systems require a transponder on board the spacecraft. This means added weight and power in the spacecraft. Since weight and power are usually at a premium, the trend has been toward the development of unified tracking and data acquisition systems in which a single carrier frequency is used in each direction for the transmission of all tracking, command, and telemetry data between the spacecraft and ground. One of the earliest unified systems was the Goddard Range and Range Rate System used for the Explorer XVIII (IMP) satellite. In general, a pulse radar type of tracking system is incompatible with a unified tracking and data acquisition system concept. The United States manned spaceflight programs of Mercury and Gemini utilized radar tracking. However, the current Apollo program for landing a man on the moon has switched to a Unified S-Band tracking system which is primarily a code ranging system. The

Goddard Range and Range Rate tracking system utilized in STADAN is primarily a sidetone ranging system.

In a code ranging system, the range to a spacecraft is determined by sending a repetitive pseudo-random ranging code to the spacecraft. The spacecraft transponder returns the continuous stream of pseudo-random code to the ground receiver. The overall code pattern is designed such that when the pattern is compared with the same pattern displaced by an integral number of bits, there is only one relative position that yields maximum correlation, and all other relative positions yield uniformly low correlation. The received code is correlated against a delayed transmitted code. The amount of delay necessary for obtaining correlation is equal to the delay in transmitting the signal to the spacecraft and back. The maximum round-trip time which can be determined without ambiguity corresponds to the total length of the code.

A sidetone ranging system determines the range to a spacecraft by transmitting to the spacecraft several discrete, coherently related subcarrier frequencies. The spacecraft transponder sends the ranging sidetones back to the ground receiver. The delay between the ground-transmitted subcarriers and transponder return subcarriers is directly proportional to the two-way range between the tracking antenna and the satellite. The lowest sidetone frequency has a wavelength that is greater than the two-way range to the satellite. The delay measurement of the lowest sidetone is used to resolve the ambiguity in the next sidetone frequency which is about 5 times higher than the lowest sidetone. The successive sidetone frequencies are in ratios of approximately 5 to 1 such that the delay reading of each sidetone frequency will easily resolve the ambiguity of the next highest frequency. The highest sidetone frequency determines the range resolution obtainable with the system.

Both the code ranging system and the sidetone ranging system have certain advantages and disadvantages. The code ranging system can generate extremely long codes, and hence can be very effective for extremely great ranges such as those encountered in deep space missions. This is one of the primary reasons why it was first developed by the Jet Propulsion Laboratory (J.P.L., 1963) for use in deep space missions. The disadvantages of the code ranging system are that the code bit rate must be very high for a ranging precision of a few meters, and the spectrum of the code covers a very wide bandwidth. A sidetone ranging system, on the other hand, uses a much lower frequency for the same range precision and the discrete ranging tone frequencies occupy a relatively small part of the spectrum. The disadvantage of the sidetone system is that the very low frequencies that would be required for interplanetary distances are difficult to handle in the electronic systems. For ranges of earth orbiting spacecraft the lowest frequency is high enough that it is not a problem. The development of sidetone ranging technique has been pioneered by the designers (Habib et al., 1964) of STADAN which has a heavy load of earth orbiting missions.

The optimum system is a combination pseudo-random code and sidetone ranging system. In such a system a ranging code is employed to resolve the ambiguity when the transit time to the spacecraft and back is greater than the period of the lowest sidetone. Such a composite system allows the maximum range resolution to be obtained from a signal of a given bandwidth while easily resolving ambiguities at distances greatly in excess of the lunar distance. Such a combined system is optimum for tracking satellites in intermediate to lunar range orbits and in tracking all phases of a complex vehicle mission involving near-earth and deep space operations.

C. Goddard Range and Range Rate System

The Goddard Range and Range Rate System (Kronmiller and Baghdady, 1965) determines the spacecraft range, range rate and angular position. The range measurement technique (Baghdady and Kruse, 1964; Fitzgerald et al., 1964) combines the advantages of sidetone and pseudo-random signals in a highly effective and versatile manner, operable either as an all sidetone system in near-earth orbital tracking or as a hybrid system for tracking more distant spacecraft. The system also combines the utilization of the two types of signals by a technique which speeds up the process of acquiring the ambiguity resolving code component in tracking spacecraft at cis-lunar and translunar distances. Doppler techniques are employed to measure range rate. The autotracking antenna position is employed to measure spacecraft angle. In addition, the system is a unified system, capable of transmitting commands and of receiving telemetry data on the same r.f. carriers.

A simplified block diagram of the GRARR system is shown in Figure 4. The system is designed for range and range rate tracking in either the S-band or the VHF frequency band. The frequencies for the VHF mode of operation are 148-150 MHz for the uplink and 136-138 MHz for the downlink. The frequencies for the S-band mode are 1750-1850 MHz for the uplink and 2200-2300 MHz for the downlink.

In the S-band mode of system operation, the S-band portion of the system is used to extract range, range rate, and angle data; and the VHF autotrack receiver and antenna is used to guide the S-band antenna in the initial spatial acquisition of the spacecraft. Initially the VHF antenna scans around the expected spacecraft position until the VHF autotrack receiver locks onto the 136-138 MHz beacon transmissions from the spacecraft. During this operation, the S-band antenna is slaved to the VHF antenna and the S-band transmitter radiates an unmodulated carrier. When the VHF antenna acquires the spacecraft, the S-band transponder is unsquelched by the S-band uplink carrier and begins transmitting. The S-band receiver then locks onto the satellite transmissions and automatically initiates the modulation of the uplink carrier with ranging tones, the S-band antenna

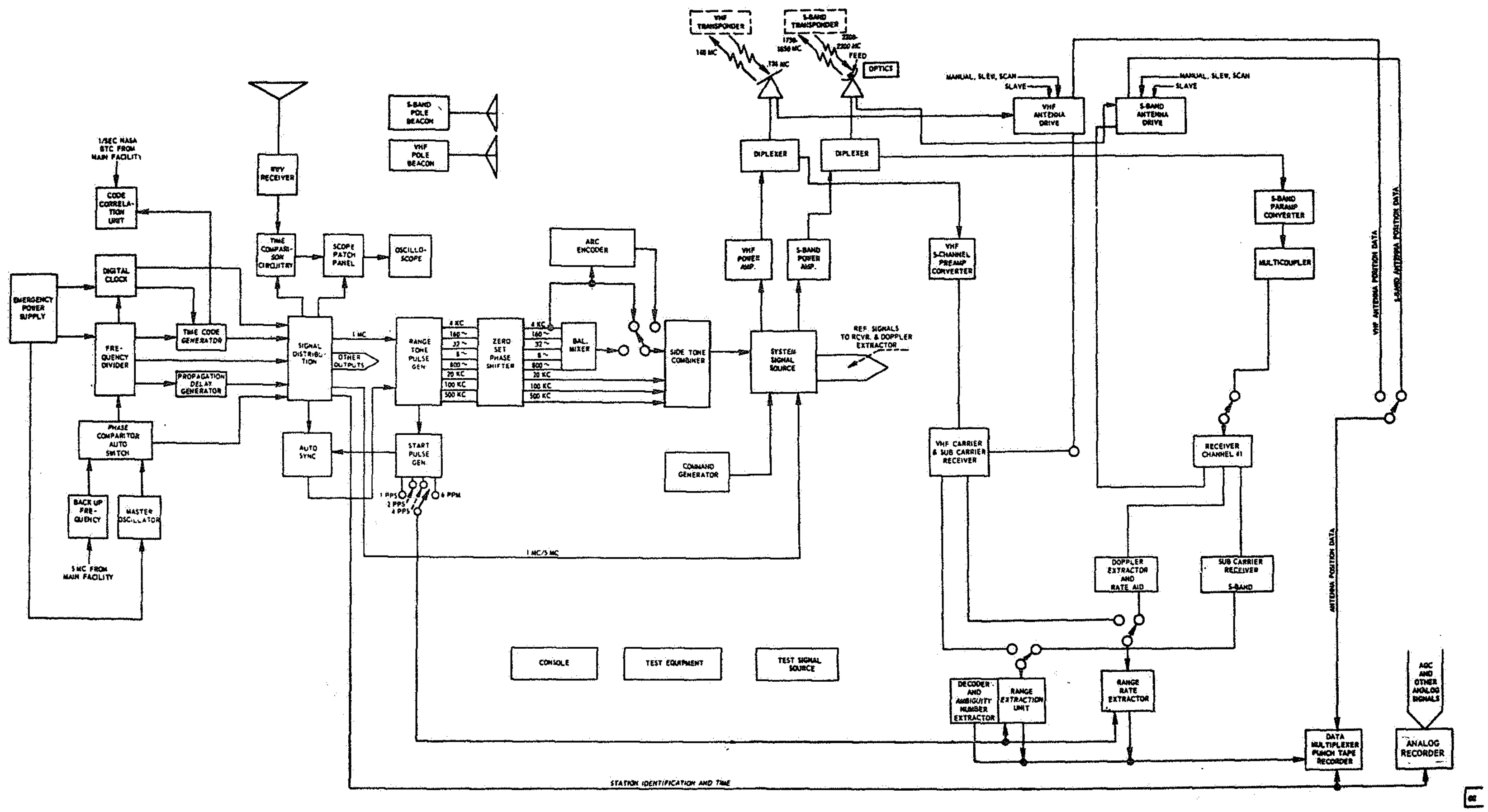

Figure 4. Goddard Range and Range Rate System block diagram.

autotrack mode of operation, and the extraction of range, range rate, and angle data.

In the VHF mode of operation, the VHF antenna scans around the expected spacecraft position until the transponder carrier frequency is acquired by the VHF ground receiver. Then the antenna automatically reverts to an autotrack mode, range tones are applied to modulate the uplink VHF carrier and the VHF receiver starts extracting range, range rate, and angle data.

Precision range measurements are accomplished by the use of ranging sidetones. The time delay between ground-transmitted sidetones and transponder returned sidetones is directly proportional to the two-way range between the tracking antenna and the satellite. The ranging sidetone frequencies are 500 kHz, 100 kHz, 20 kHz, 4 kHz, 800 Hz, 160 Hz, 32 Hz, and 8 Hz. Thus, except for the last tone, successive frequencies are in a 5:1 ratio. Any one of the three highest tones may be selected by the operator as the highest resolution tone for a mission, based upon the available transponder bandwidth or other considerations. The lower frequency tones are used to resolve range measurement ambiguities. The lowest sidetone available, 8 Hz establishes an unambiguous range to approximately 18000 km. For greater ranges the hybrid ranging mode is employed. In the hybrid ranging mode an ambiguity resolving pseudo-random code having a length of 32385 bits is bi-phase modulated on the 4-kHz sidetone. The code bit rate is 4 kHz. The ambiguity resolving code is made up of two sub-codes of 127 and 255 bits respectively. In this mode, the unambiguous range is approximately 1.2 million km.

The phase coherent ranging sidetones are generated in the range tone pulse generator. 'Reference' pulses of 4 pps, 2 pps, 1 pps, or 5 ppm are also generated. The ranging sidetones and 'Reference' pulses are generated in a fully clocked digital divider chain using a 1-MHz frequency standard signal as an input. Each of the "Reference' pulses is coincident with the positive-going zero crossings of the higher tones. A 'Reference' pulse, along with a zero crossing of the highest tone in use, is used to generate a 'Start' pulse that marks precisely the time of transmission of an all zero-phase condition for all the tones.

Prior to transmission, the ranging tones pass through the zero-set phase shifter unit. This unit enables individual and combined phase shift of the ranging tones so that the individual tones can be phase or time shifted with respect to those used to generate the start pulse. In this way an adjustable bias can be applied in the range time measurement to calibrate out the effect of fixed equipment time delays and differential time delays between tones.

For transmission, the four lowest ranging sidetones are complemented on the high side of the 4-kHz tone to produce sum frequencies of 4800; 4160; 4032;

and 4008 Hz. These frequencies are then combined with the higher sidetones of 20 kHz, 100 kHz, and 500 kHz for modulating the transmitter. This system eliminates modulation components close to the carrier which could degrade carrier acquisition and tracking.

Both the VHF transmitter and the S-band transmitter carrier frequencies are synthesized from the 1-MHz/5-MHz precision frequency source in the system signal source subsystem. This unit also provides all reference and local oscillator frequencies for the receiver as well as the carrier frequencies for the transmitters. The system signal source also contains the phase modulators in which the composite ranging tones from the sidetone combiner are modulated upon the carrier frequencies. This unit also provides coherent frequency samples of the carrier frequencies for use by the doppler extractor.

The sum of the ranging tones phase modulates the uplink carrier. The signals received at the spacecraft transponder are heterodyned down to pre-assigned subcarrier frequencies by mixing with a multiple of a locally generated reference signal. For S-band, the reference oscillator frequency, f_0, is used in a double conversion to translate a signal of received doppler shifted uplink carrier frequency, Kf_t, to a subchannel at $48 f_0 - Kf_t$. Three subchannel frequency bands are used, centered at 1.4 MHz, 2.4 MHz and 3.2 MHz, corresponding to three different ground transmitter frequencies. This allows the transponder to be used by 1, 2, or 3 ground stations simultaneously. Each transponder subchannel contains bandpass amplifiers, limiters, and a squelch gate. The outputs of the subchannels in use are summed and used to phase modulate the downlink carrier. The squelch gates keep the unused subchannels from modulating the downlink carrier with pure noise. The downlink signals is PM/PM. Figure 5 shows the resultant spectra at the inputs and outputs of the S-band transponder. It should be noted that the transponder transmit frequency is derived from the reference oscillator f_0 which was used to generate the local oscillator frequencies for the double conversion to subcarriers. This technique enables the downlink signal to be usable by the ground stations to extract two-way doppler for range rate measurement, free of the effects of the transponder reference oscillator instabilities, and without requiring the spacecraft oscillator to establish phase-lock with the incoming signal.

The VHF transponder is similar in operation to the S-band unit, except that it is only capable of one channel operation with 20 kHz as the highest ranging tone frequency. This is primarily due to the lack of bandwidth and frequency allocation in the VHF region. In the VHF transponder the reference oscillator translates the received signal to 1 subchannel at $Kf_t - 13f_0$. The transponder output frequency is $12/13\ f_t$. The spectra of the VHF uplink and downlink signals are shown in Figure 6.

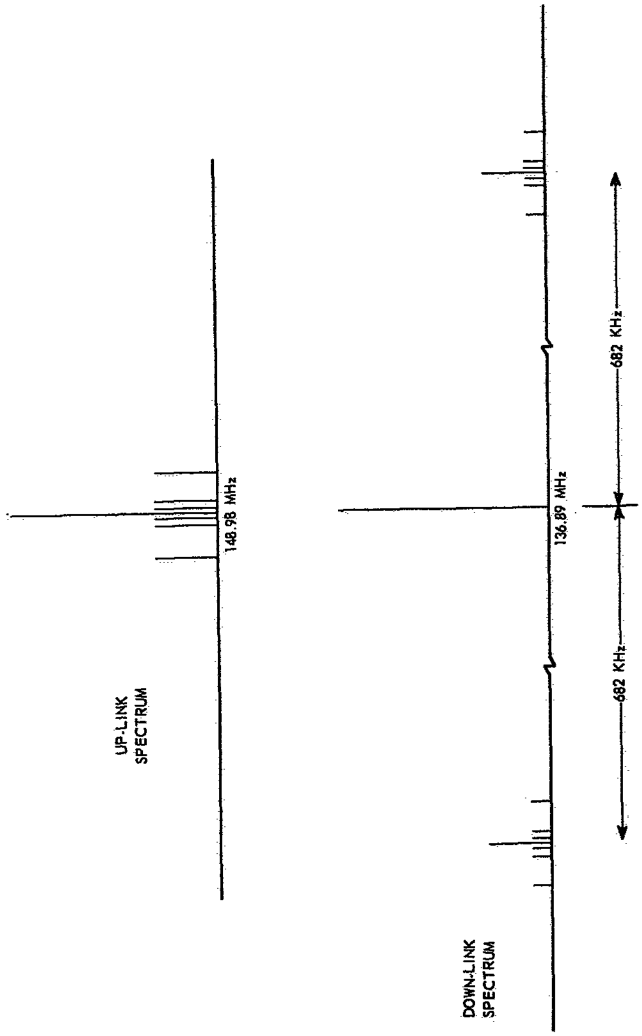

Figure 6. VHF-band spectra of Goddard Range and Range Rate System uplink and downlink signals.

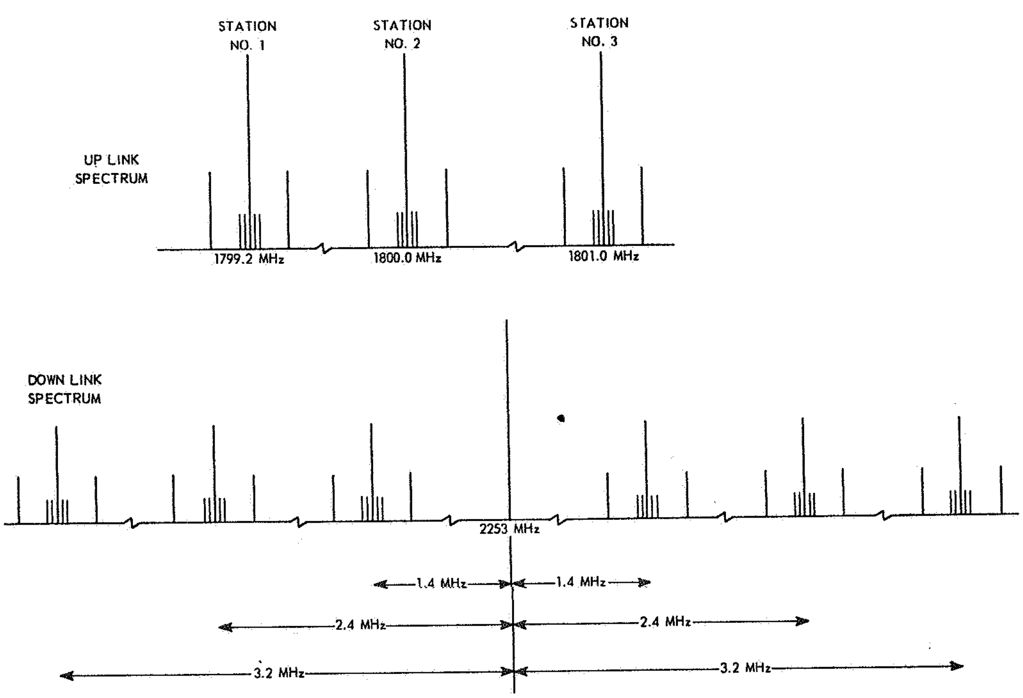

Figure 5. S-band spectra of Goddard Range and Range Rate System uplink and downlink signals.

The transponder can also serve as a telemetry transmitter for the spacecraft. The ranging function is energized by a command signal that allows the ranging modulation to be placed on the carrier. Thereafter the presence of the 4 kc ranging tone holds the transponder in the ranging condition until the tones are turned off, at which time the transponder reverts back to a simple telemetry transmitter.

The ground receiver uses an extracted carrier reference to shift the desired portion of the downlink r.f. spectrum down to a zero frequency center, filters the desired tones, and sends them to the Range Extraction Unit. The Range Extraction Unit regenerates clean tones that are phase coherent with the received tones in the following manner. The highest tone in use (100 kHz for example) is used to drive a digital divide chain that regenerates all of the other tones (i.e., 20 kHz, 4 kHz down to 8 Hz). The reconstructed 20 kHz will be either in phase with the received 20 kHz or some multiple of $360/5 = 72°$ out of phase with it. The phases of the digitally generated 20 kHz and the received 20 kHz are compared, and the digitally generated 20 kHz is stepped in phase until a zero phase difference is indicated. Once the 20 kHz tone is locked, the 4 kHz tones are synchronized in the same manner. This same process is used to phase synchronize all of the digitally reconstructed tones. The use of this digital tone extraction technique makes it possible to switch off lower frequency tones after acquisition, since only the highest tone is required to drive the digital divide chain.

The measurement of range is performed in the following manner. As the sidetones are transmitted, a time interval 'Start' pulse is generated by the coincidence of the 'Reference' pulse and a positive-going zero crossing of the highest tone in use. The 'Start' pulse marks precisely the time of transmission of an all zero-phase condition for all of the sidetones. After return via the spacecraft transponder, the received sidetones are applied to the Range Extraction Unit for regeneration of clean tones phase coherent with the received sidetones as explained above. The positive-going zero crossings of the regenerated tones are then used to generate a 'Stop' pulse that marks the instant of reappearance of the all zero-phase condition for all of the received sidetones. The time separation between the 'Start' and 'Stop' pulses is the round trip transit time to the spacecraft transponder. This time separation is measured by counting the number of 100-MHz periods enclosed within it. The measurement resolution is 10 nanoseconds.

When the Ambiguity Resolving (AR) code is used in conjunction with the sidetone system, the AR code is applied only after the tone system is completely acquired and tone ranging 'Start' and 'Stop' pulses are being generated. Once the tone system is acquired, the minor tones are removed from the transmitter and replaced with the AR-code-modulated 4-kHz subcarrier. The first tone 'Start'

pulse is used by the AR decoder control logic to simultaneously stop the AR decoder and set its register contents equal to the contents of the transmitter AR encoder. When the tone 'Stop' pulse is received by the control logic, the AR decoder is started, using the doppler shifted 4 kHz from the digital tone extractor as a clock. Thus, the AR decoder has been offset in time from the AR encoder by the ambiguous two-way transit time to the spacecraft, as measured by the tone system. The AR decoder will then be either in phase with the received demodulated code, or time-shifted from it by an integral number of 1/8 sec intervals. The acquisition process now consists of making a trial correlation between the AR decoder and the received AR code and if correlation is not indicated, stepping the AR decoder by 500 bits (1/8 sec) and testing again for correlation. This process is repeated until correlation is achieved. The ambiguity number counter receives a pulse from the decoder logic circuit each time the AR decoder is stepped 500 bits, keeping track of the number of 8-Hz periods involved. Provision is made for an operator to start the acquisition sequence at any range ambiguity slot, allowing maximum use to be made of any a priori range information.

The method used to shift the AR decoder in 500 bit steps is worthy of description here. It is desired to delay the AR decoder 500 bits, which would require deleting pulses at a 4-kHz rate if done in a conventional manner. Another way of achieving the same thing is to shift the code sequence forward through a whole sequence period minus 500 bits. Since the sequence used here is made up of two short subsequences, it can be shown that by shifting the 255 bit subcode ahead 10 bits, and the 127 bit subcode ahead 8 bits, the composite code is shifted ahead 31885 bits producing the desired 500 bit delay. Furthermore, since we are now adding pulses rather than deleting them, they can be added at a fast rate (100 kHz) and the entire shift can take place between 4-kHz clock pulses, thus minimizing the AR code shift time.

After correlation has been achieved and the hybrid system is completely locked to the return signal, the number in the ambiguity number counter indicates the number of full 1/8 sec periods in the round trip time to the spacecraft. The hybrid system now provides a continuous periodic check on this number so that it will automatically be updated when the spacecraft range changes to a new ambiguity slot.

Range rate is determined from the two-way doppler shift of the uplink carrier frequency. In order to measure this doppler shift, it is necessary to maintain coherence of the uplink frequency through the transponder and back to the ground receiver where it is compared in frequency against a continuing sample of the uplink frequency in the range-rate extraction unit. The range-rate extraction unit measures doppler by determining the elapsed time of a preset number of cycles of the sum of the doppler shift plus a known frequency offset.

The uplink carrier, f_t is generated from the ultrastable 5-MHz frequency standard. This 5-MHz signal is frequency multiplied in a frequency synthesizer to produce the uplink carrier. This signal is amplified, and radiated to the transponder, arriving as Kf_t where K is the one-way doppler coefficient representing the doppler shift in frequency on f_t resulting from the transponder range rate, $\dot{R}$, and is given approximately by $K = 1 + \dot{R}/c$, for $\dot{R}/c << 1$. In the S-band system, the signal received at the spacecraft is processed by the transponder to generate a subcarrier $(48 f_0 - Kf_t)$ which is then used to phase modulate a 60 f_0 downlink carrier. This signal is transmitted down to the ground receiver where it is received with a doppler shift because of transponder motion relative to the tracking station. The signal at the ground receiver has a carrier frequency of $60 K' f_0$ and a subcarrier frequency of $(48K' f_0 - KK' f_t)$ corresponding to an original uplink frequency f_t. The objective of the ground receiver and doppler extractor circuit is to extract $(KK' - 1) f_t$, the coherent two-way doppler on f_t.

The receiver carrier loop phase-locks a voltage controlled oscillator to the incoming carrier, providing a reference at $K' f_0$. The carrier loop phase detector also yields the subcarrier. A subcarrier loop phase locks a voltage controlled oscillator to this subcarrier, producing a reference signal at $(48K' f_0 - KK' f_t)$. The doppler extractor takes these two signals, the transmitter reference $f_t/48$, and a bias frequency f_b, and combines them to produce $(f_b + (KK' - 1) f_t)$. The desired $(KK' - 1) f_t$ term is obtained on a bias frequency that is greater than the maximum expected negative doppler shift so that a zero frequency crossover is avoided. The measured frequency is higher or lower than the bias frequency, depending upon whether the spacecraft is approaching or receding from the tracking station. The doppler frequency together with its sense is determined later in the process of data reduction by subtracting the bias frequency from the measured frequency. The maximum two-way doppler is about ± 10 kHz at VHF frequencies and ± 130 kHz at S-band frequencies. The nominal bias frequencies are 30 kHz for VHF and 500 kHz for S-band. The bias frequencies are derived from the transmitted carrier frequency such that $f_b = Bf_t$, where $B = 1/3600$ for S-band and $B = 1/5000$ for VHF. The doppler extraction process cancels out any instability of the transponder oscillator, f_0, provided that these instabilities are properly tracked by both carrier and subcarrier phase-locked loops.

The range rate extraction unit measures the time interval associated with N_0 cycles of the bias-plus-doppler signal. A pulse from the time standard unit starts the gating in of cycles of bias-plus-doppler to the N_0 cycle counter. The first positive zero crossing of the first gated bias-plus-doppler cycle generates a 'Start' plus which starts the time interval unit counting pulses of a reference frequency f_r. This frequency reference is derived from the transmitted carrier frequency, f_t, by the relation $f_r = qf_t$, where q is 1/180 for S-band and 1/15 for VHF. The gating of the bias-plus-doppler signal continues until a count of

'N_0' has been reached in the N_0-Counter. At the positive going zero crossing of the '$N_0 + 1$'th bias-plus-doppler cycle, a 'Stop' pulse is generated which turns off the gate and the reference frequency counter. The count, N, of f_r cycles in the time interval unit can be expressed as

$$N = \frac{N_0 f_r}{\left[f_b + (KK' - 1) f_t\right]} = \frac{N_0 q}{\left[B + (KK' - 1)\right]}$$

The two-way doppler is computed from the measured N and the preselected N_0. Note that the derived range rate is independent of the transponder frequency f_0 and the transmitted frequency f_t.

The VHF range rate measurement system is functionally the same as in the S-band system. The major difference is that the VHF carrier and doppler frequencies are lower, and consequently lower values of N_0 and f_r are used.

The Goddard Range and Range Rate System has been in operation since 1963. The VHF system has been used to track all of the IMP series of spacecraft. The original VHF system was designed to have a standard deviation of range measurement of better than 50 m at a received signal strength of -124 dbm. The system performance exceeded the design goals. The IMP data (Kronmiller and Baghdady, 1965; Kronmiller and Zillig, 1967), has a standard deviation of about 20 m for a -124 dbm signal strength.

At the present time both the VHF system and the S-band system are being upgraded as part of a switch of the S-band system to the new operating frequencies described earlier in this paper. (The original S-band system operated with an uplink frequency of 2271 MHz and a downlink frequency of 1705 MHz.) The improved VHF system is expected to have a range accuracy of 15 m.

The intercomparison tracking tests conducted on the GEOS spacecraft have shown that the old S-band Range and Range Rate System had a standard deviation of range measurement of about 8 m. The new system improvements are expected to reduce this uncertainty to about 2 m.

The range rate measurements with the old VHF system have a standard deviation of about 0.3 m/sec. A range rate data from the original S-band system has a standard deviation of approximately 0.03 m/sec. These performance numbers are expected to be the worst case performance numbers for the new improved systems.

D. Apollo Unified S-Band System

The Unified S-Band System was developed to provide reliable tracking and communications to the Apollo manned spacecraft at lunar distance (Varson, 1965). The unified systems approach was used in order to reduce the amount of equipment required aboard the spacecraft.

The tracking and communications with the Apollo spacecraft during the lunar missions are provided by three primary facilities, employing 85-foot antennas spaced at approximately equal intervals of longitude around the earth (Goldstone, California; Madrid, Spain and Honeysuckle Creek, Australia) to provide a continuous coverage of the lunar missions. Three of the Deep Space Instrumentation Facilities at approximately the same locations are equipped to serve as backup to the primary stations. Each of these facilities, both primary and backup stations, are equipped to track and provide communications with both the lunar excursion module and the command module simultaneously.

In addition to the stations with the 85-foot antennas, a number of other stations employing 30-foot antennas are also required in the network. These systems are needed for launch coverage and for coverage in between the gaps of the three lunar stations when the Apollo spacecraft is in close earth orbit. Four land stations (Cape Kennedy, Florida; Grand Bahama, B.W.I.; Antigua; and Bermuda) and one instrumentation ship are required to provide continuous USB coverage from launch through insertion. Seven land stations (Canary Island; Guaymas, Mexico; Corpus Christi, Texas; Ascension Island; Carnarvon, Australia; Guam; and Hawaii) and two additional instrumentation ships are required to complete the USB system coverage requirements. In addition to these stations (Figure 7) the Manned Space Flight Network also includes one reentry ship and eight instrumented aircraft.

There are several variations to the basic USB system: the single and dual 30-foot system, the primary and backup 85-foot antenna systems, and the single and dual instrumentation ships. However, the same general systems concept is utilized for tracking in each one of the systems. The USB system that is used with the 85-foot primary antenna systems will be used to illustrate the system design concepts. The system block diagram is shown in Figure 8. The design of the USB system is based on the coherent doppler and pseudo-random range system (Lindley, 1965; J.P.L., 1963) which has been developed by the Jet Propulsion Laboratory. The USB system is a hybrid system in that the pseudo-random range code is used to obtain the range to a resolution of 300 m of one-way range, and then finer range resolution is obtained by phase locking the receiver to the shortest code (2 bits) and measuring the phase difference between the transmitted code and the received code thereby using the shortest code as a ranging sidetone. This is done to a resolution of one-half a bit period which

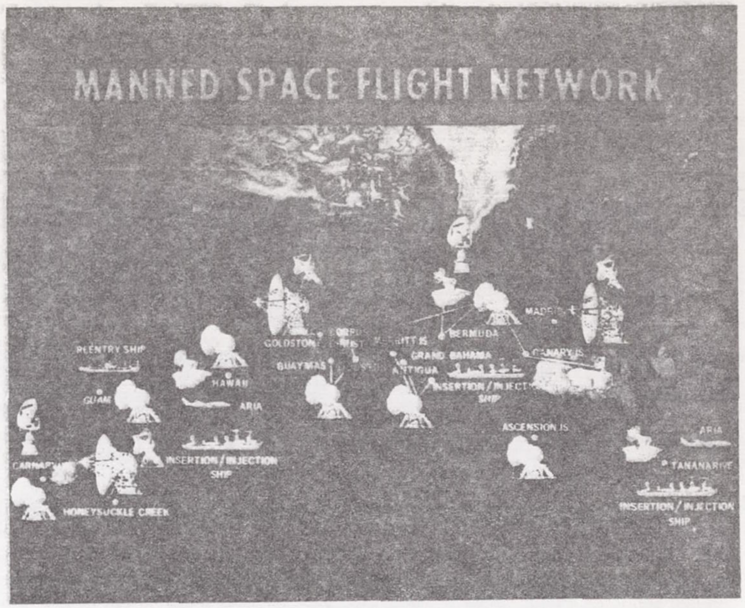

Figure 7. The NASA Manned Space Flight Network configuration for Apollo tracking and data acquisition.

corresponds to 75 m of range. Once ranging code acquisition has been accomplished the system switches from tallying every one-half bit period to tallying every 16th S-band doppler cycle. This improves the resolution to approximately ± 1 m.

A single carrier frequency is utilized in each direction for the transmission of all tracking and communications data between the spacecraft and ground. The voice and up-data are modulated onto subcarriers and then combined with the ranging data. This composite information is used to phase-modulate the transmitted carrier frequency. The frequency spectrum is shown in Figure 9. At the spacecraft, the carrier is received and coherently transponded (Hood, 1965; Kuykendall, 1965) by the ratio of 240/221 and then retransmitted to the ground station. In the transponder, the subcarriers are extracted from the r.f. carrier and detected to produce the voice and command information. The ranging signals,

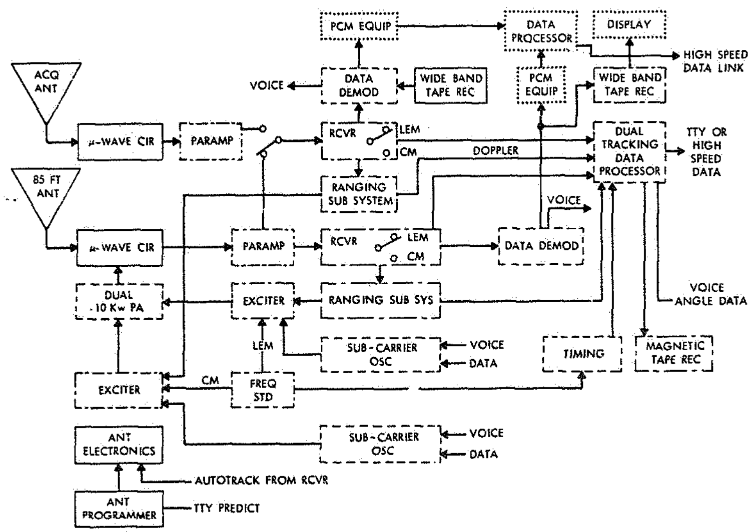

Figure 8. Apollo USB System diagram for 85-foot antenna facility primary stations.

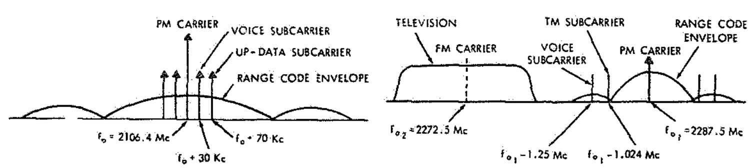

Up-link spectrum.

Typical down-link spectrum.

Figure 9. USB system frequency spectrum for Command and Service Module.

modulated directly onto the carrier, are detected by the wide-band phase detector and translated to a video signal. The voice and telemetry data to be transmitted from the spacecraft are modulated onto subcarriers, combined with the video ranging signals, and used to phase modulate the downlink carrier frequency. A transponder transmitter can also be frequency modulated for the transmission of television information or recorded data instead of ranging signals.

The basic USB system has the ability to provide tracking and communications data for two spacecraft simultaneously, provided they are within the beam width of the single antenna. Two sets of frequencies separated by approximately 5 MHz are used for this purpose. In addition to the primary mode of communications, the USB system has the capability of receiving data on two other frequencies. These are used primarily for the transmission of FM data from the spacecraft. The uplink frequencies are in the 2090–2120 MHz band, and the downlink frequencies are in the 2270–2300 MHz band.

The ranging code (Lindley, 1965) used in the USB system has a total length of 5456682 bits. This code is made up of 5 repetitive shorter subcodes or code components whose designations and lengths in bits are: CL code component of length 2 bits, X code component of length 11 bits, A code component of length 31 bits, B code component of length 63 bits, and C code component of length 127 bits. This code provides a maximum unambiguous range of slightly more than 800000 km. It is possible to acquire the total code by acquiring the components individually in turn which reduces the number of correlation reading required to 232. Note that the 2-bits CL component is not acquired by digital means, but rather by the process of locking up the clock loop in the ranging receiver.

The range determination process is shown diagrammatically in Figure 10. The ranging signals transponded by the Apollo spacecraft are received at the ground station. This downlink modulated carrier is coherently translated to an i.f. frequency of 10 MHz in the phase lock receiver. This 10-MHz ranging output signal consists of the pseudorandom ranging code modulated on the 10-MHz i.f. frequency. This modulation occupies a wide spectrum containing significant sideband components as far as 2 MHz from the carrier. This spectrum is applied to a wideband phase detector. The reference signal for the phase detector is a 10 MHz frequency, modulated with the receiver code. The receiver code is identical to the transmitted pseudorandom range code except that it does not contain the two-bit clock (CL) code. The phase detector differences the two signals, producing an output signal which always contains some energy at the clock frequency. The amplitude of this clock output is directly proportional to the degree of correlation between the code received from the spacecraft and the receiver code. The inner phase-lock loop, or clock loop, is initially locked up to the

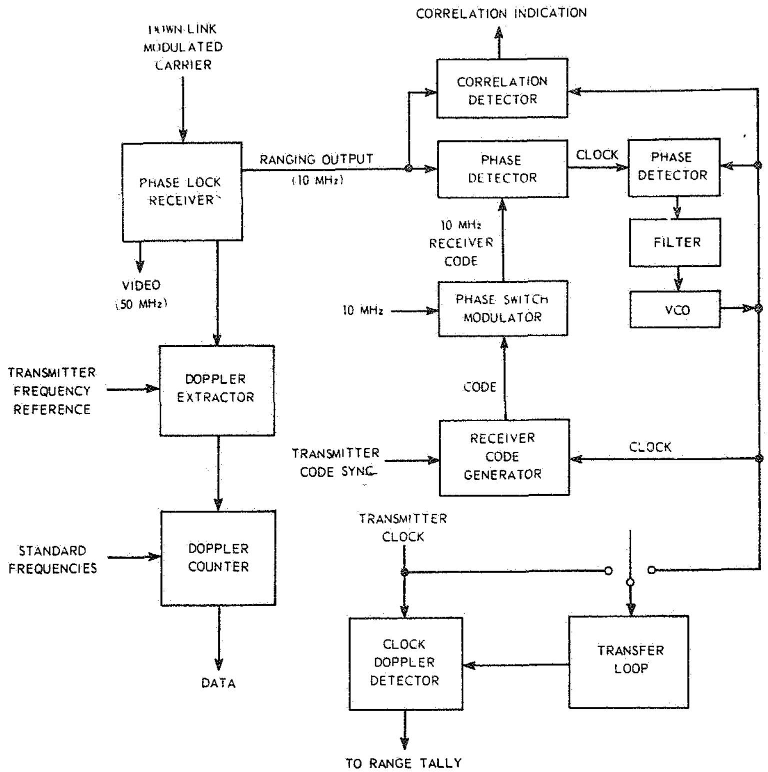

Figure 10. USB system tracking functional diagram.

incoming clock component which it subsequently tracks. The outer loop, or code loop, matches the received code to the receiver code. This matching is accomplished by digitally shifting the components of the receiver code and measuring the correlation indication at each relative shift position until a maximum is obtained. The total ultimate shift of the receiver code from its initial phase is a measure of the initial range at the start of acquisition, with a resolution of one clock cycle. Each shift of each component in the process of acquisition is noted by adding the appropriate number of range units into the range tally whenever such a shift is made. At the start of acquisition of the range code, the receiver coder is code-synchronized to the transmitter-coder.

The received clock code is delayed with respect to the transmitted clock code by some unknown integral number of clock-code periods plus a delay equal to some unknown fraction of a clock period. A clock transfer loop is provided to help determine the value of the fractional period in order to determine range more precisely than one clock code length. At the start of range acquisition, the input to the transfer loop is connected to the transmitter clock. The inputs to the clock doppler detector are then identical and there is no output. The range tally is set to zero range units. The transfer loop is now switched to the receiver code. As the transfer loop tracks into the phase without loss of lock, the doppler detector keeps track and causes tallying of range numbers in accordance with what appears to be a slight spacecraft motion. This then corrects what would otherwise have been an error in range corresponding to the fractional clock cycle delay. Increments in range resulting from spacecraft motion are detected, clock cycle by clock cycle, in the clock doppler detector and are continually tallied in the range tally. Clock doppler tallies are made every one-quarter of a clock cycle, for a resolution of 75 m of range. Once acquisition has been accomplished the system automatically switches from tallying every one-quarter clock doppler cycle to tallying every sixteenth S-band doppler cycle. This improves the resolution by a factor of 72 to ± 1 range unit or approximately ± 1 m of range.

Once range has been acquired, it is possible to disable the full code modulation and modulate the carrier instead with the two-bit clock code only. There is no further need for the code, the clock component alone being responsible for keeping the clock loop in lock. The advantage of changing from full code to clock code lies in the fact that this not only cuts down on the required sideband power, but also limits the spectral distribution of ranging frequencies to two single spectral lines, 496 kHz above and below the carrier frequency.

The doppler extraction function (Bunce, 1965) is performed as follows. The received signal from the spacecraft transponder which appears at the ground receiver input has a frequency of $(240/221)\, f_t + D$. The quantity D is the two-way doppler frequency, and has a maximum value of about 160 kHz at earth escape velocity. The receiver is phase locked to this received frequency, and receiver reference signals containing frequencies coherently related to the received frequency are applied to the doppler extractor. Similarly, frequencies coherently related to the transmitted frequency are also applied to the doppler extractor. Within the doppler extractor the transmitter references are suitable combined and shifted coherently to simulate the 240/221 ratio occurring in the spacecraft. The resulting signal is functionally differenced with the receiver references to yield the doppler frequency D. Finally, this frequency is added to a 1.0 MHz bias frequency from the frequency standard, and the resulting biased doppler, or range-rate signal, is supplied to the doppler counting system. The bias frequency is applied to the doppler frequency in order that the signal to be counted in the doppler counter never goes through zero frequency.

The doppler counter (Hocking, 1965) has two modes, destruct and non-destruct. In the destruct mode, the 100-MHz counter performs a high-resolution time measurement of a predetermined number (N) of biased-doppler cycles. The measurement is made in the following manner. A pulse from the time standard system opens a gate and the first positive zero crossing of the first gated biased-doppler cycle is shaped and advances the N-counter to state 1. This transition turns the 100-MHz counter on, which starts immediately counting 100-MHz pulses (synthesized, 1 MHz input from the time standard system). The gating of the biased-doppler signal continues until the count of 'N' has been reached in the N-counter. At the positive going zero crossing of the 'N + 1'th cycle, the gate and the 100-MHz counter are turned off. The result is a 100-MHz counting operation for precisely the period of time between positive going zero crossings of the first and 'N + 1'th biased-doppler cycle. The advantage of N-counter techniques is briefly that high resolution measurements (10 nsec) are available with short measurement periods.

In the non-destruct mode the same operation takes place, except that 'N' is very large and the off pulse never occurs to turn off the gate. The counting operation continues without disturbance or reset throughout the spacecraft tracking period. The advantage of the non-destruct technique is that a continuous, undisturbed doppler measurement is made with no data gaps such as exist in the destruct mode. In the non-destruct mode, the N-counter contents are transferred to storage each 0.1 sec or once per second.

The performance of the USB tracking system is summarized as follows. The overall system ranging accuracy is approximately ± 15 m. Ranging accuracy is limited by drifts and instabilities in ground and space loops. The minimum range acquisition time is 1.6 sec at strong signal levels and can go as high as 30 sec at lunar distances in the MSFN configuration. The range-rate accuracy of the system is better than 3 cm/sec.

E. Laser Ranging Systems

The newest and the most precise ranging system used in space exploration today is the laser pulse ranging system. This is a pulse radar system at optical frequencies. A high powered laser transmits a very short pulse of optical radiation toward the satellite. Retrodirective optical reflectors on the spacecraft return the light pulse to the ground along the same path. The ground receiver located next to the transmitter detects the received pulse. The time interval between the emission and the detection is a measure of the range to the satellite.

There are now six satellites in orbit which have arrays of cube-corner retroreflectors designed for laser ranging. These are the U.S. satellites Beacon

Explorer B and C (Explorers 22 and 27), GEOS 1 and 2 (Explorers 29 and 36), and two French satellites D-1C and D-1D. The reflector arrays (Plotkin, 1964) are composed of accurately polished fuzed silica cube-corners, which reflect incident radiation back towards its source, with relatively high efficiency. A photograph of the reflector array for the Beacon Explorer satellites is shown in Figure 11. The retrodirective arrays are fairly inexpensive and lightweight. Passive transponders of this type have a big advantage for precise ranging because they do not introduce any transponder biases in the range determination. One of the main error sources for radio ranging systems is the transponder bias error introduced in the spacecraft.

Since the first Beacon Explorer B satellite was launched into orbit in October 1964, a number of organizations (Plotkin et al., 1965; Snyder et al., 1965; Bivas and Morael-Courtois, 1966; Iliff, 1965; Lehr et al., 1967) have been employing

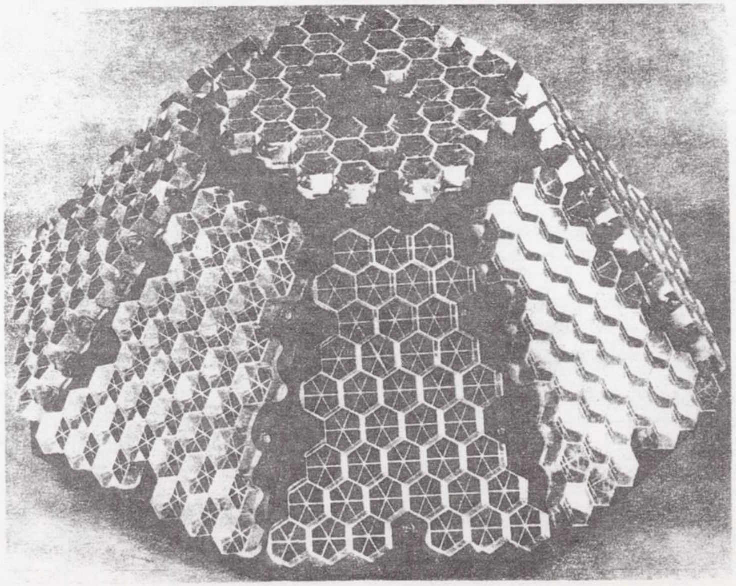

Figure 11. Optical reflector array on Beacon Explorer B.

pulse ruby lasers for precise satellite tracking. The possibility of generating extremely short laser pulses coupled with the passive transponder on the satellites indicated that very precise ranging was possible with this technique. This technique has become a very valuable tool for improved orbit determination and satellite geodesy.

Figure 12 is a photograph of the laser ranging system developed by Johnson et al. (1967), at the Goddard Space Flight Center. The system consists of a ruby laser transmitter, a receiver-detector system, a precise tracking pedestal to point the laser transmitter and receiver, and a ranging and data-control system. The laser transmitter is a water-cooled ruby laser which incorporates a combination rotating prism and bleachable liquid 'Q'-switch with an output beam sampling unit and 10-power collimating optics. The divergence of the transmitted laser beam is 1.2 milliradians. The laser transmitter is operated at 1 pulse per second. Each pulse normally has an energy between 0.9 and 1.2 J, with a rise time of 5 to 8 nsec and a half-width of 12 to 15 nsec.

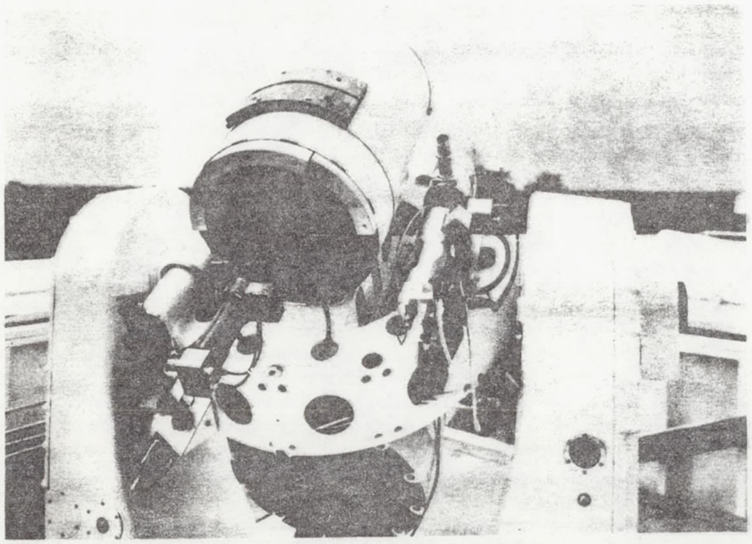

Figure 12. Goddard pulse ruby laser ranging system (Johnson et al., 1967).

The receiving antenna is a 40-cm aperture, 762-cm effective focal length Cassegrain telescope. The receiver detector system is housed in a light tight compartment at the focal point of the telescope. An adjustable iris determines the field of view. An interference filter and an EMI 9558 A photomultiplier detector follow the adjustable iris.

Both the laser transmitter and the receiving system are mounted together on the same tracking pedestal. The pedestal for this system is a modified Nike-Ajax radar mount. The elevation axis was modified to allow mounting of the laser transmitter and the 40-cm aperture receiving telescope. A 32-power view finder, used for visual observation of the satellites, is mounted parallel to the laser and the receiving telescope on the top portion of the elevation axis. Seventeen-bit shaft encoders on both azimuth and elevation are used in digitally controlling the tracking pedestal according to both predicted satellite orbit positions and visual corrections.

The operation of the Goddard laser ranging system is diagrammed in Figure 13. The time code generator sends 1 pulse per second to the laser power supply to trigger the start of a laser pulse. The rotating prism 'Q'-switch is not synchronized with the 'on-time' pulse. Therefore the laser fires from 8.5 to 11 millisec after the command time. The precise time of the firing of the laser is detected with a laser beam monitoring unit. The pulse from the monitor starts a 1000-MHz time interval range unit. The monitor pulse also starts the range-gate system which turns on the receiver photomultiplier avalanche detector during a short interval about the time at which the predicted signal is expected to arrive. The detected received pulse stops the time interval unit. The resolution of the time interval unit is equivalent to a range resolution of 15 cm.

The Goddard pulse laser ranging system has been used extensively for the GEOS satellite program of intercomparison and calibration of the network satellite tracking systems. Figure 14 shows the laser range residuals from a short arc orbit solution during a typical pass. The plotted points are differences between individual laser observations and the range calculated from an analytical orbit adjusted to a least variance fit. The r.m.s. scatter about this smooth curve is about 1 m. This is an indication of the precision of the laser ranging system, as distinguished from accuracy. The system accuracy has been determined by calibrating the system against carefully measured distances on the ground, and by conducting simultaneous ranging of the GEOS spacecraft with several independent ranging systems collocated at the same site. Early in 1968 the laser tracking system was moved to Wallops Island, where it was in close proximity to an FPQ-6 radar, an FPS-16 radar, a SECOR station, and a photographic camera. All of these systems were used to track GEOS 2 simultaneously, so that their intercomparison would not suffer from the uncertainties in station

LASER TRACKING SYSTEM BLOCK DIAGRAM

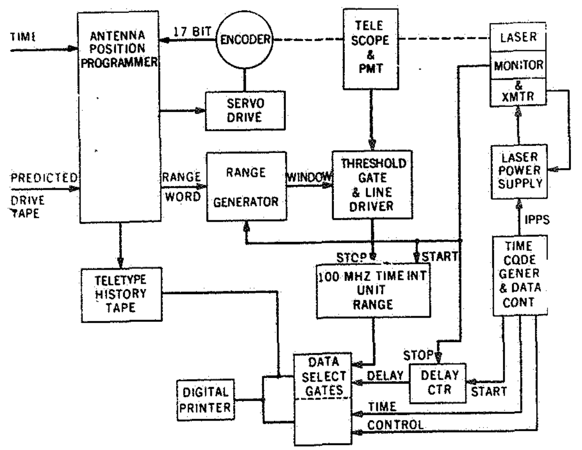

Figure 13. Goddard laser ranging system diagram (Johnson et al., 1967.

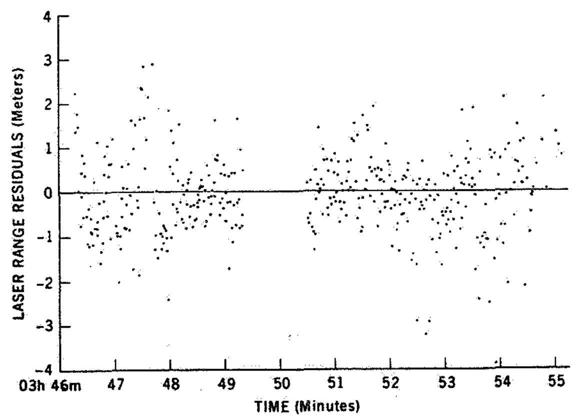

Figure 14. Goddard laser system range residuals from a short-arc orbit solution during a typical pass of GEOS B on June 6, 1968.

location and orbit dynamics. The analysis of all of the intercomparison data taken over a period of several months did not reveal any systematic bias in the laser tracking data greater than 1 m. It was concluded that the laser ranging system accuracy is the order of 1 m.

3. FREQUENCIES FOR TRACKING AND DATA ACQUISITION

The performance of a tracking or data acquisition system is strongly dependent upon the signal-to-noise ratio of the system. In general the better the signal-to-noise ratio the better the system performance. For example, Figure 15 is a plot of the bit error probability for PSK and FSK telemetry as a function of the normalized signal-to-noise ratio (energy per bit/noise power density). This curve of increase in error probability as a function of decreasing signal-to-noise ratio is rather typical for tracking and data acquisition systems. Consequently the system designers strive to obtain high signal-to-noise ratios.

Consider the case of a spacecraft transmitting telemetry to be received at a ground station. The signal power, P_r, received at the ground station receiver is given by the equation $P_r = P_t A_s A_g / \lambda^2 R^2$, where P_t is the r.f. power radiated by the spacecraft transmitter, A_s is the effective area of the spacecraft antenna, A_g is the effective area of the ground antenna, λ is the r.f. wavelength, and R is the range between the ground antenna and the spacecraft antenna. Most spinning spacecraft utilize an omnidirectional antenna in order to have uniform signal strength received by the ground station. The effective area of an omnidirectional antenna is $A_s = \lambda^2/4\pi$. Therefore the power received from a spacecraft with an omnidirectional antenna is $P_r = P_t A_g / 4\pi R^2$. Therefore if an omnidirectional antenna is used on the spacecraft, the signal power received at the ground station is independent of the frequency of transmission. The situation is quite different, however, for a stabilized spacecraft that can direct an antenna beam toward the ground station. In this case, the antenna area A_s can be maintained the same irrespective of frequency. Then the power received at the ground station is proportional to the square of the frequency of transmission. This indicates that it is advantageous to use higher frequencies when it is possible to use a directable antenna aboard a spacecraft.

Most earth orbiting spacecraft are of the spin stabilized type, or are stabilized (to orient the scientific sensors) in such a manner that the spacecraft antenna must have a fixed beamwidth. The effective area of an antenna of fixed beamwidth is also proportional to $\lambda^2/4\pi$, and consequently the signal power received is also independent of wavelength for the constant beamwidth antenna on the spacecraft.

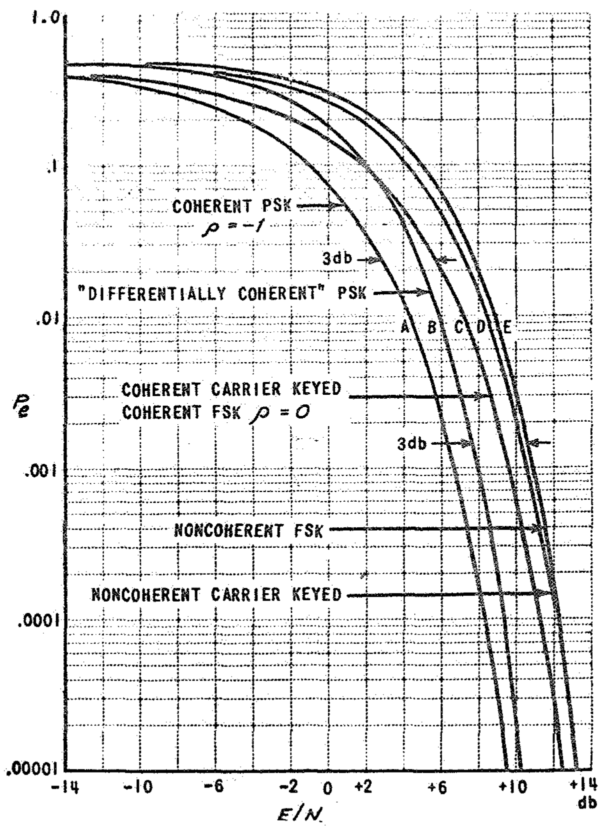

Figure 15. Probability of error for phase shift-keyed (PSK) and frequency shift-keyed (FSK) telemetry (Lawton, 1958).

The main sources of noise in a telemetry system are the sky noise of *galactic*, radio star, solar and lunar radiations plus black body radiations from the lossy atmosphere; antenna noise of radiation from the earth received through the backlobes of the antenna plus radiations from resistive losses in the antenna

system; and the receiving system noise. The system noise power P_n is commonly given in terms of an equivalent system noise temperature T_n (Dicke, 1946) by the equation $P_n = kT_n\Delta f$ where k is Boltzman's constant and Δf is the frequency bandwidth. Some typical values of galactic noise temperatures, receiver preamplifier noise temperatures, and antenna noise temperatures are plotted in *Figure 16 as a function of frequency*. The sky noise at the lower frequencies is predominantly galactic and radio star noise (Ko, 1958; Horner, 1960). This galactic and radio star noise drops off very rapidly with increasing frequency, and it is negligible at frequencies above 2000 MHz. The atmospheric

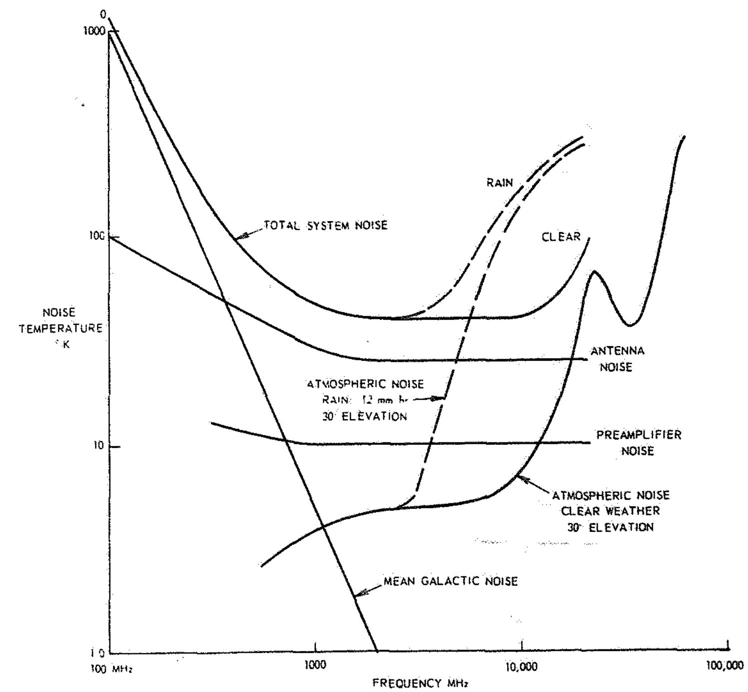

Figure 16. Total data acquisition system noise temperature and noise temperature components due to galactic radiation, atmospheric losses, rain losses, antenna noise, and preamplifier noise as a function of frequency.

absorption is primarily due to oxygen and water vapor (Hogg, 1959). This begins to make an appreciable contribution to the system noise at frequencies above 2000 MHz. The atmospheric noise curve given in Figure 16 is for a 30° elevation angle. The noise temperature at higher elevation angles are slightly less than those shown in the curve due to the decrease in the path length through the atmosphere. Similarly lower elevation angles would have higher noise temperatures because of the increase in path length. Another factor is the effect of rainfall. During a rain storm, the atmospheric noise temperature is considerably higher at high frequencies because of attenuation due to the rain (Benoit, 1968), as shown in Figure 16. The preamplifier noise temperature is that of a low-noise maser preamplifier. It is common practice to achieve noise temperatures of 10° or better with liquid helium cooled maser systems. Parametric amplifier technology is beginning to produce noise temperatures in the region between 10° and 20°K. The antenna noise temperature curve corresponds to a well-designed cassegrain 85-foot parabolic antenna system for frequencies above 1000 MHz. Below 1000 MHz the cassegrain antenna system loses its effectiveness because of the small size of the cassegrain subreflector in terms of the wavelength of the radiation, and consequently there has to be a transition to a focal point feed at the very low frequencies. The total system noise (which is the sum of the sky noise, the antenna noise and the preamplifier noise) is in excess of 1000° at 100 MHz and drops down rather suddenly to temperature in the neighborhood of 40° at 2000 MHz. In clear weather it stays relatively constant from 2000 MHz up to 10000 MHz and then begins to rise as the frequency is further increased. During rain, the system temperature begins to rise above 3000 MHz.

Just about all of the spacecraft which have been orbited or are soon to be launched have spacecraft antennas based on omnidirectional or fixed beamwidth pattern requirements. Ground antennas of about the same aperture are used for 100 to 10000 MHz. The relative signal-to-noise ratio as a function of frequency is given in Figure 17 for the typical case of a fixed beamwidth spacecraft transmitting antenna, a constant receiving antenna aperture, and system noise temperatures from Figure 16. The highest all-weather signal-to-noise ratio is at about 2000 MHz. This was one of the reasons for selecting the 2000 MHz band for the Deep Space Network, the Apollo Unified S-Band system, and the Goddard Range and Range Rate System.

As a matter of history, the vast majority of scientific spacecraft orbiting the earth are utilizing the VHF band for tracking and data acquisition. The reason for this becomes apparent only when one considers the practical engineering design of the spacecraft transmitting system. Most of the spacecraft are spin stabilized spacecraft which do not have the capability of directing an antenna towards a ground station. A spinning spacecraft will present almost all aspects to the data acquisition ground stations. Thus the spacecraft antenna must approximate an omnidirectional antenna. A turnstile antenna has a pattern close to omnidirectional if the ground station can receive both orthogonal polarizations.

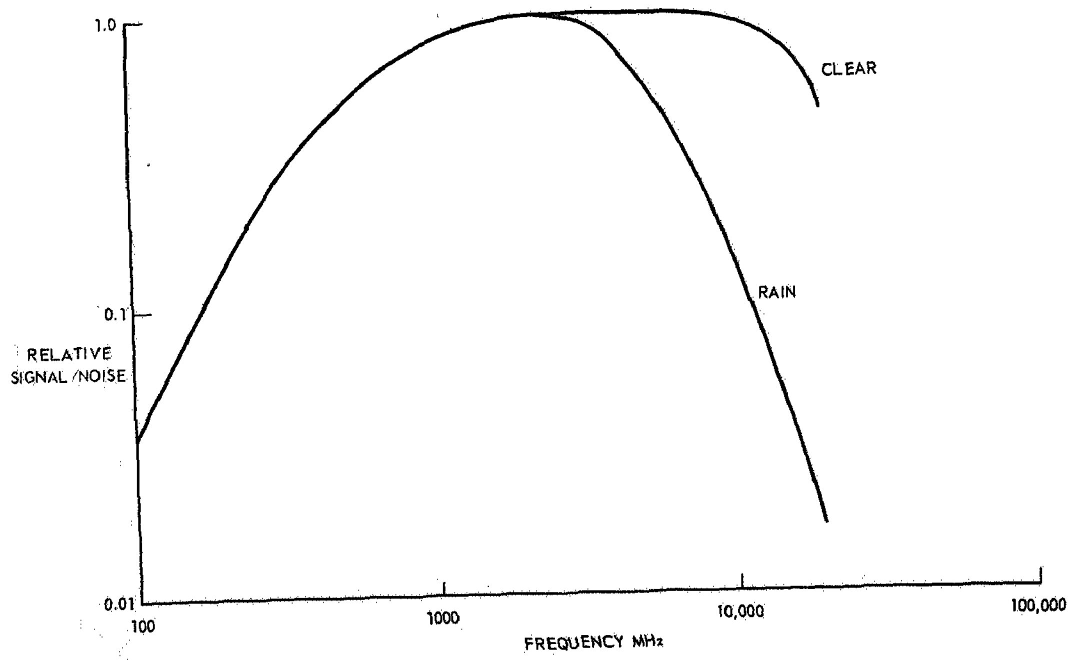

Figure 17. Relative received signal-to-noise ratio as a function of frequency for a fixed beamwidth spacecraft transmitting antenna, a fixed ground receiving antenna area, and system noise temperature from Figure 16.

The turnstile consists of 2 crossed one half wavelength dipoles energized with currents of equal magnitude but in phase quadrature. This produces right circular polarization in the front axial direction, left circular polarization in the rear axial direction, and both right and left circular polarizations for off-axis directions. The turnstile dipoles must be appreciably larger than the spacecraft in order to have the desired antenna pattern. Thus long wavelengths of the order of several meters must be used. This type of antenna has been quite effective in the 136-MHz telemetry band. At frequencies between 1000 and 10000 MHz, all spacecraft are several wavelengths in size. A half-wavelength turnstile cannot be used on spacecraft at these high frequencies. At the present time there is no antenna in existence which produces a good omnidirectional pattern when mounted on a spacecraft that is many wavelengths in size. Antennas designed for such situations invariably have many deep nulls in the antenna pattern. This of course creates a very difficult problem for the transmission of continuous telemetry data. This is the primary reason that most spin stabilized spacecraft are still operating in the VHF band.

Another factor is the efficiency and reliability of the spacecraft transmitter. For several years, very efficient, reliable, and lightweight solid state transmitters have been available for medium power use in the 100-MHz to 150-MHz region. It was only three years ago that advances in transistor technology produced efficient 400-MHz solid state transmitters. Only in the last year have manufacturers produced 2000 MHz power transistors capable of generating 5 W of r.f. power. Up until now S-band transmitters have used the less reliable vacuum tubes.

The spacecraft antenna and transmitter problems forced most of the systems designers to utilize the VHF band for tracking and data acquisition. However, the future trend will be toward utilization of the high-frequency bands between 1500 and 10000 MHz. The recent switch of the frequencies for the USA manned flight missions up to the 2000-MHz band is an example.

All of the deep space probes and a few of the earth orbiting spacecraft have used the higher frequencies. The Nimbus weather satellite was attitude stabilized to always direct its cameras toward the earth. Therefore it could use an antenna with a 90° beamwidth oriented toward the earth. This type of antenna is relatively simple to design at the higher frequencies. The transmission of weather pictures from Nimbus requires several MHz and bandwidth. The 136-MHz and the 400-MHz bands are only 1 MHz wide. Only the high-frequency bands have enough bandwidth for the transmission of video pictures. Thus Nimbus utilized the 1700-MHz band for the transmission of the weather data. The early Nimbus flights used a vacuum tube transmitter, but the new flights will have the more efficient solid state transmitters.

A stabilized spacecraft, such as Nimbus, may have a failure in the stabilization system. Such a failure could cause the spacecraft to tumble much in the manner of a spinning spacecraft. Under this condition it is necessary to have an omnidirectional spacecraft antenna in order to regain control of the spacecraft through the use of the command link. For this reason the Nimbus spacecraft uses the 148-MHz band for sending commands and the 136-MHz band for narrow band telemetry from the spacecraft. It is common practice for spacecraft utilizing the higher frequency bands to also have a limited VHF capability for backup operations in case of an emergency.

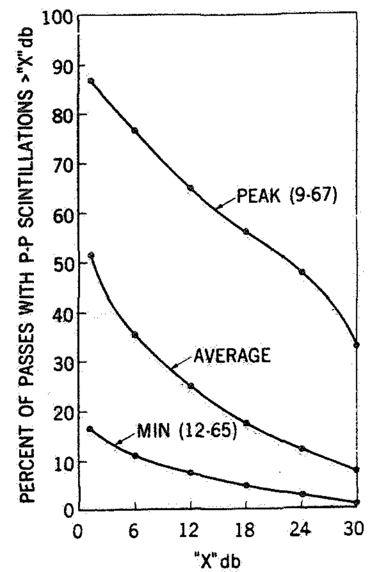

Figure 18. Amplitude distribution of peak-to-peak scintillation of 136 MHz satellite signals due to auroral ionospheric disturbances at Fairbanks, Alaska (Coates and Golden, 1968).

Another frequency dependent factor to be considered is that of the propagation characteristics of the atmosphere. In utilizing the VHF band, spacecraft designers must take into consideration the ionospheric disturbances of 136-MHz signals. High ionospheric activity is observed in the auroral zone and in a zone at the magnetic equator. Serious disruptions of VHF telemetry, command, and tracking operations are experienced in both of these zones (Coates and Golden, 1968). The observed distributions of peak-to-peak amplitudes of scintillations of 136-MHz satellite signals received in the auroral zone at the NASA data acquisition station at Fairbanks, Alaska are shown in Figure 18. The middle curve is the average distribution for the total period of January 1965 through September 1967. The upper curve is the distribution for the month of peak activity, September 1967, and the lower curve is the distribution for the month of lowest activity, December 1965.

For most satellites, a peak-to-peak scintillation of 6 db is not a significant problem because it is the same order of magnitude as the signal variations due to spacecraft antenna pattern. However, when the scintillation is 12 db or higher most telemetry acquisition is degraded. At levels of 18 db of scintillation, the telemetry is extremely poor and the data acquisition receiver drops out of lock occasionally. The scintillation levels above 12 db are a serious operational problem to a satellite project. The data presented in Figure 18 shows that for the past three years at Fairbanks, Alaska, on the average 25% of the satellite data acquisition passes had signal scintillations of 12 db or greater peak-to-peak. During the most disturbed month, 65% of the passes had scintillations greater than 12 db.

Fremouw (1966) and Zonge et al. (1967) have correlated the scintillations with all-sky camera photographs of auroral activity and TV camera images of the sky in the direction of the antenna pointing. These comparisons clearly show that the VHF telemetry scintillations are concurrent with visible auroral disturbances. Both the visible aurora and the satellite signal scintillations are dependent upon solar activity. Figure 19 shows the measured correlation between the number of passes with scintillations greater than 12 db and the monthly mean of the 10.7-cm solar flux as reported by Ottawa (ESSA, 1966-67).

The ionospheric disturbances experienced in the region of the earth's magnetic equator have a much different character than those observed in the auroral zone. The disturbances at the magnetic equator have a very strong diurnal

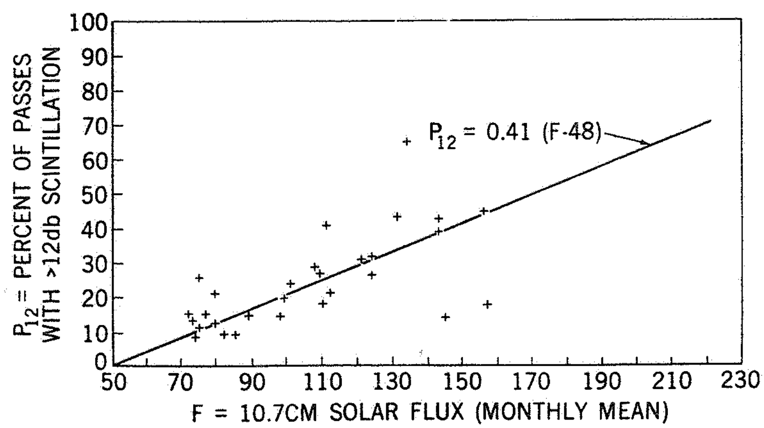

Figure 19. Measured correlation between 136 MHz satellite signal scintillations and 10.7-cm solar flux (Coates and Golden, 1968).

variation. This shows up on the records of the Minitrack system. The ionospheric disturbance creates considerable scintillation in both amplitude and phase. During the nighttime hours a very sizeable number of Minitrack passes are completely destroyed by the ionospheric disturbances. Figure 20 is a plot of the percent of lost Minitrack passes for the Lima, Peru, station for the month of March 1967. The percent of Minitrack passes lost as a function of the hour started to increase just after sunset and went up to a maximum of almost 70% close to local midnight and then dropped down again to a negligible amount shortly after sunrise. The total number of passes that were lost during the month amounted to approximately 14% of all passes attempted. The highest ionospheric activity is observed at Lima which is on the magnetic equator; lesser activity is observed at Quito, Equador, and Santiago, Chile which are respectively North and South of the magnetic equator. The measured seasonal variations for Lima, Quito, and Santiago are given in Figure 21. The disturbance to 136-MHz signals peaks to a maximum in the spring and fall corresponding to the solar equinox.

The Minitrack system measures the angle of arrival with two different sets of interferometer antennas, one oriented North-South and the other oriented

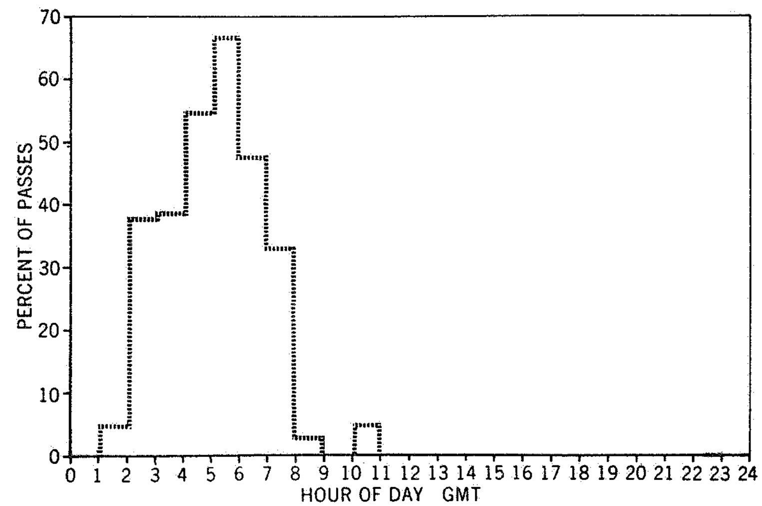

Figure 20. 136 MHz Minitrack passes missed by hour of day for Lima, Peru in March 1967 due to ionospheric propagation disturbances (Coates and Golden, 1968).

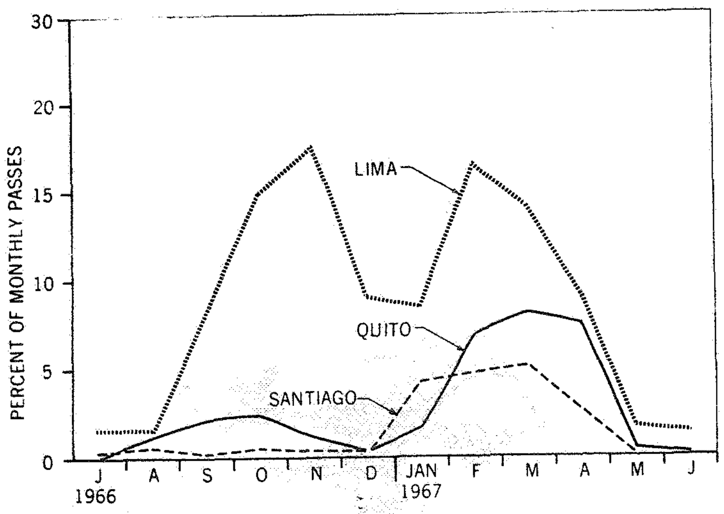

Figure 21. 136 MHz Minitrack passes missed by month due to ionospheric propagation disturbances (Coates and Golden, 1968).

East-West. During conditions of ionospheric disturbance, the East-West baseline is much more severely disturbed than the North-South baseline. This is consistent with a model of the ionosphere consisting of densely ionized streams aligned North-South with the magnetic field of the earth.

The natural question to ask is what can be done to circumvent the degradation due to ionospheric disturbances. Fremouw (1966) has shown that the auroral scintillations are due to scattering in the ionosphere and that the optical depth for scattering is inversely proportional to the square of the frequency. Scintillation is thus much less at higher frequencies. This was determined from the analysis of several years of records of simultaneous observations at multiple frequencies. At a frequency of 1700 MHz, ionospheric scintillations were observed on only two passes out of 15000. Those two satellite passes had scintillations of only 1 db peak-to-peak. Satellites in polar orbits such as the operational weather satellites which make very heavy use of the Northern station at Fairbanks, Alaska, should use the higher frequencies in order to maintain the operational reliability demanded of the mission. Similar considerations of the

equatorial ionospheric disturbances lead to the conclusion that higher frequencies should be used when reliable spacecraft tracking, command, and data acquisition are important.

Space diversity is another technique for combating the severe effects of ionospheric disturbance. Interferometer measurements during auroral scintillations have been analyzed by Fremouw (1966) to determine the size of the ionospheric disturbance elements. He has shown that if two antennas are placed at a distance greater than 300 m, the probability is very high that the scintillations received at the two antennas will not be correlated. The data of Golden (1968) and Kent and Koster (1966) indicate that the same is true for the equatorial ionospheric disturbances. Under these conditions, the outputs of the two antennas can be combined to effectively cancel the deep scintillation nulls.

Another way of avoiding serious disturbance by ionospheric propagation is to locate the tracking and data acquisition stations at mid-latitudes away from the magnetic equator and the auroral zones. It is an extremely rare occurrence when a mid-latitude station experiences ionospheric scintillations of the order of 12 db.

4. DATA ACQUISITION

A. Antennas

As discussed earlier, the functions of tracking and data acquisition for an orbiting spacecraft are so similar that the trend is to the use of unified systems for both functions. Thus the antennas used for tracking and data acquisition have the same general characteristics, and the same antenna may be used for both functions.

At the present time, NASA satellites which are supported by STADAN are transmitting at frequencies in the 136-, 400-, and 1700-MHz bands. As indicated earlier, several of the satellites send low data rate telemetry at 136 MHz and simultaneously transmit high data-rate telemetry in either the 400- or 1700-MHz bands. When spacecraft are launched with the new S-band range and range rate frequencies, the antennas will require the capability of receiving the 2200-MHz band. A paraboloidal antenna is a natural choice for operating over such a wide frequency range. Figure 22 is a picture of one of the NASA 85-foot diameter paraboloidal antennas at Rosman, North Carolina. In total, STADAN has five 85-foot antennas and five 40-foot paraboloidal antennas equipped with feeds for 136-, 400-, and 1700-MHz band reception. The locations of these antennas are shown in the STADAN map, Figure 1. The Santiago, Chile STADAN station has a 30-foot diameter Cassegrain paraboloidal antenna for the new frequencies of the Goddard Range and Range Rate system.

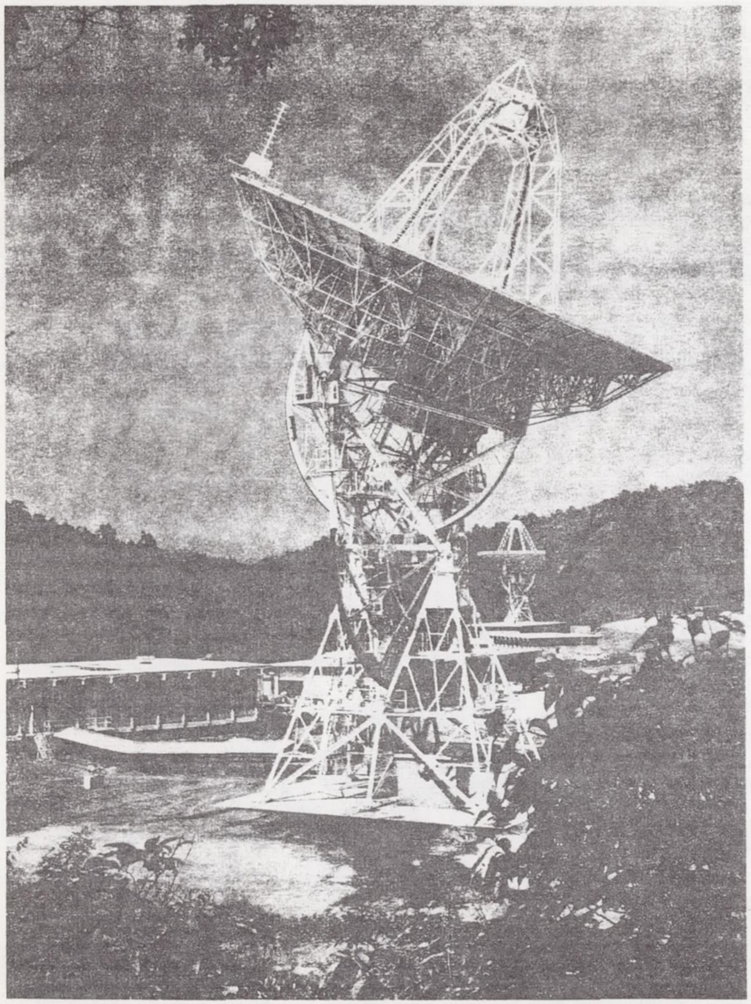

Figure 22. NASA 85-foot diameter paraboloidal antenna at the STADAN station, Rosman, North Carolina.

STADAN is designed to handle as many as 50 spacecraft in orbit at the same time. In order to handle such a workload, each station has several data acquisition links. A link (Filipowsky and Muehldorf, 1965) is defined as the string of electronics systems required for data acquisition from one satellite. The ground station part of a telemetry link consists of the telemetry antenna, receiver, demodulation equipment, telemetry data handling equipment, data transmission system, and data recording systems. A command link consists of the command antenna, command transmitter, and the command encoder. Each STADAN station has several telemetry links and command links which enables them to acquire data from several satellites simultaneously.

Since the majority of the scientific satellites use only 136 MHz for data transmission, most of the STADAN ground stations have several additional data acquisition antennas for that band only. The sky temperature is so high at VHF that gain is the dominant factor in the antenna figure of merit. Arrays generally have much higher gains than paraboloids with the same physical aperture areas. Thus arrays are used predominantly in the VHF band. Figure 23 is a photograph of the 136-MHz automatic tracking antenna (Lantz and Thibodeau, 1967) used in the NASA Satellite Tracking and Data Acquisition Network. It consists of an array of yagi elements. It has a gain of 22 db, and receives two orthogonal polarizations simultaneously for polarization diversity.

The antennas utilized for tracking and data acquisition at frequencies of 1800 MHz and higher are generally of the Cassegrain paraboloidal type of design. As discussed earlier a very low-noise antenna system is required in order to achieve the low total system noise temperature possible in the 1800- to 10000-MHz region of the spectrum. A considerable reduction in antenna temperature can be obtained by reducing the antenna spillover lobes and the back lobes which look at the earth. Sidelobes near the main beam are not as critical because they are looking at cold sky. The Cassegrain reflector antenna, as shown in Figure 24, is used extensively because it has very low back and spillover lobes. The reasons for the low level of lobes in the rear direction can be from the geometry. The feed is completely shielded in the rear hemisphere and the feed pattern beyond the hyperbolic subreflector is in the forward direction. This increases the sidelobes close by the main beam but greatly reduces the spillover lobes at large angles to the main beam. Illumination beyond the edge of the paraboloid is greatly reduced because the pattern of the hyperbolic subreflector has a relatively sharp drop at the edge of the paraboloid. Thus the back lobes of a cassegrain antenna are very low.

An important practical advantage of the Cassegrain antenna is that the feed is back at the main antenna structure. In the USB system, the antenna is used for both transmitting and receiving. Thus both the transmitting equipments and the low-noise preamplifier systems (such as cryogenically cooled parametric

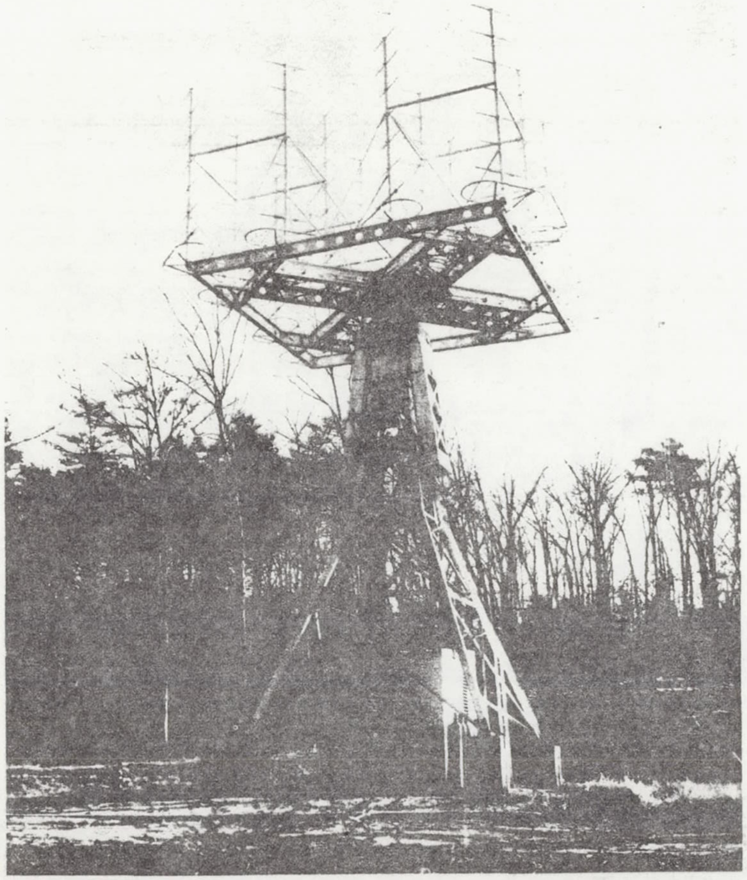

Figure 23. 136 MHz automatic tracking telemetry antenna, NASA STADAN.

amplifiers) are located next to the feed. These tend to be large and heavy. This weight easily can be supported by the main antenna structure but it would be difficult to support at the focal point of the paraboloid, as would be required with a focal point feed.

Another advantage of the Cassegrain configuration is that higher antenna efficiencies are possible with a Cassegrain feed system than with a focal point feed. Potter (1963) has developed a horn feed with very low sidelobes which obtains very high efficiency in Cassegrain antennas. He used a conical horn excited in the throat region in both the dominant TE_{11} mode and the higher order TM_{11} mode. These two modes are excited in the horn aperture with appropriate relative amplitude and phase to suppress the sidelobes and to equalize the beamwidths to match the Cassegrain subreflector. This same principle has been used in the design of the Apollo USB Cassegrain monopulse antenna feeds and for the S-Band Cassegrain feeds for the JPL Deep Space Network stations.

The antenna mount axis configuration is unique to antennas used for tracking and data acquisition from earth orbiting spacecraft. A satellite tracking antenna must be capable of tracking through all parts of the sky above a few degrees elevation and have its best tracking capability around the zenith position. The X-Y mount (Rolinski et al., 1962) was developed specifically for space data acquisition antennas, and is used extensively in the NASA Space Tracking and Data Acquisition Network and the NASA Manned Flight Network. The X-Y mount has the primary axis placed horizontally, and the secondary axis placed orthogonal to the primary axis such that the secondary axis is horizontal when the antenna is pointed at the zenith. The primary axis is called the X-axis and the secondary axis is called the Y-axis. The axis motions of an X-Y antenna mount are shown in Figure 24. All two-axis antenna mounts have a gimbal lock position in the direction of the primary axis. Gimbal lock is the failure of the mount to follow a moving satellite because the required angular shaft velocity exceeds the capability of the drive system. The relation between the primary shaft speed $\dot{\theta}$ and the velocity of the satellite during a tracking operation is $\dot{\theta} = V_\theta \sec \phi / R$ where V_θ is the θ component of the satellite velocity in a plane perpendicular to the primary axis, ϕ is the angle between the satellite position and the plane normal to the primary axis and R is the range. For a satellite passing directly overhead, the angle ϕ is zero, sec ϕ is unity and the shaft speed is equal to the V_θ/R. For tracking in the direction along the primary axis, however, the angle ϕ approaches 90°, the sec ϕ approaches infinity and the shaft velocity required also goes to infinity. When the required angular velocity of the primary axis exceeds the capability of the servo drive system, the antenna can no longer track the spacecraft. This inability to track in the direction of the primary axis is referred to as gimbal lock. Satellite tracking requires the absence of gimbal lock zones above elevation angles of a few degrees. The X-Y-axis configuration places the gimbal-lock positions on

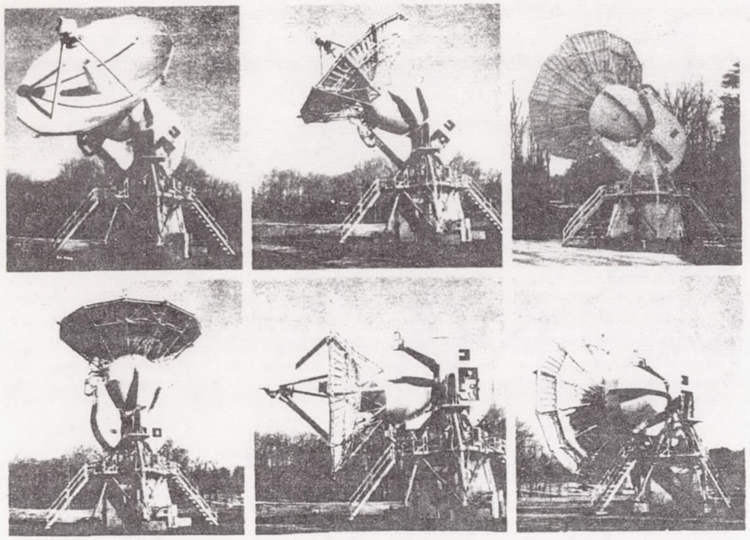

Figure 24. 30-foot Cassegrain antenna, Apollo Unified S-band system.

the horizon. Antenna sites selected for low interference are usually valleys surrounded by hills which shield the antenna from man-made interference. These hills prevent data acquisition at the horizon. Hence, the gimbal lock position at the horizon does not cause any loss of data.

Another feature of the X-Y mount is that the relation between the axis rotation and the velocity of the satellite is complementary to the relation between the angular velocity of the satellite and the maximum elevation of the satellite position. The peak angular velocity of a satellite during a pass is a maximum for a zenith pass and decreases with passes of decreasing maximum elevation angle. As a result, the highest X-axis shaft speed is essentially independent of the meridian elevation angle of the satellite pass for meridian elevation angles above 20°. Consequently the X-Y mount will track satellites throughout the entire sky above a few degrees elevation with moderate shaft velocities and accelerations. In addition, the zone of maximum tracking capability matches the zone of highest satellite angular velocity.

The X-Y-mount has another advantage. It is not necessary to use slip rings, rotary r.f. joints, or extensive cable wrap systems to bring out the r.f. and power lines. Each axis travels only ± 90°; thus a simple flexible section of cable is all that is needed to go across either axis.

All space tracking and telemetry antennas use autotrack in order to accurately follow the spacecraft across the sky. This is important in the very early phases of a mission such as launch phase or immediately after launch during which the orbit of the spacecraft is not known precisely enough to program an antenna. The STADAN and the Manned Space Flight Network antennas use monopulse autotrack (Rhodes, 1959; Cohen and Steinmetz, 1959). With monopulse, the full antenna gain is available for the reception of tracking and telemetry signals, and simultaneously the monopulse system provides continuous tracking information to the antenna servo system. Multimode feed designs have made possible fairly high efficiencies for tracking and data acquisition with the monopulse autotrack capabilities.

All of the STADAN data acquisition antennas have provisions for polarization diversity operation. This is required because most of the satellites in orbit are spin stabilized, and consequently the polarization of the signal received from the spacecraft is continuously changing as a function of the spin of the spacecraft. It is not possible for a fixed polarization in a ground antenna to match the incoming polarization from a spinning spacecraft for the duration of the satellite pass. Consequently all STADAN antennas have the capability of receiving on both of the two orthogonal linear polarizations or on both of the two orthogonal circular polarizations.

B. Polarization Diversity Receiving Systems

It is well known from vector theory that the polarization of any signal can be represented by two orthogonal polarization components of the appropriate phase and amplitude. Thus, by receiving the two orthogonal components and adding them together in proper phase relationship, one can completely reconstruct the original signal. Phase tracking techniques make it possible to receive the maximum signal strength for all aspects of a spacecraft. This is the principal for polarization diversity in space data acquisition.

Polarization diversity requires two receiver channels, one for each polarization. Early systems utilized two independent phase-lock receivers but this had the drawback that the receivers tended to drop out of lock during the extreme signal fades. Laughlin (1963) and DiLosa (1966) developed a diversity phase-lock receiving system which utilizes a common lock loop for both channels, and thereby avoids the loss of lock when one channel is below threshold. The block diagram of the diversity lock loop is shown in Figure 25. The frequency tracking

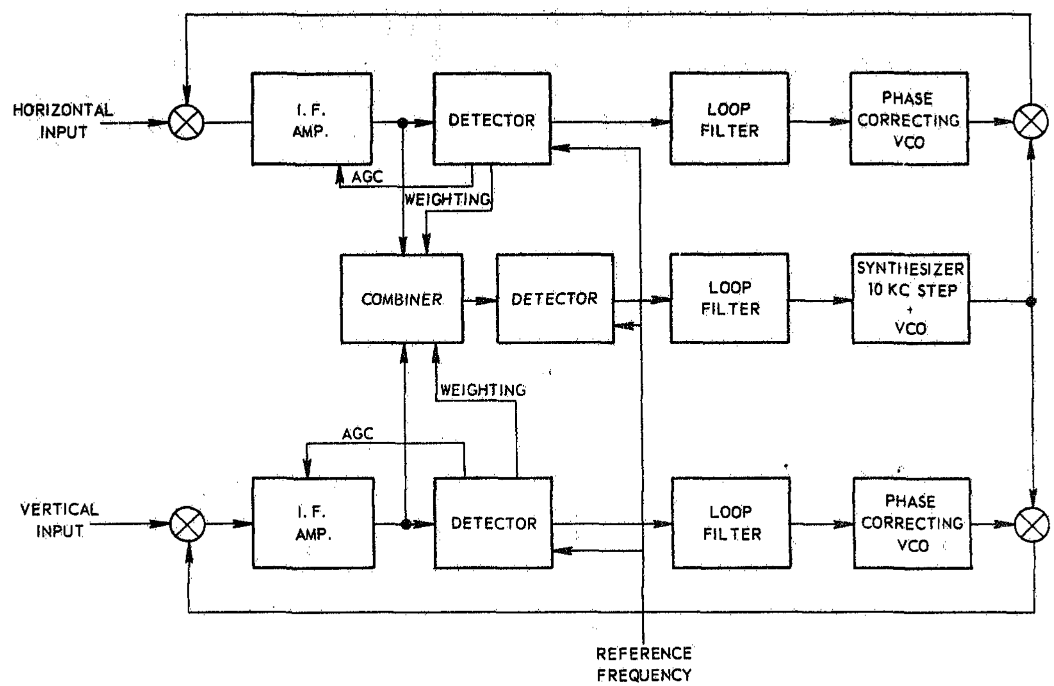

Figure 25. Locked loop for polarization diversity.

is accomplished in the primary phase-lock loop in the center of the diagram. Working in conjunction with this primary loop are two secondary phase-lock loops shown at the top and the bottom of the diagram. The secondary phase-lock loops act as electronic phase shifters to correct the phase of the signals from the horizontal and vertical polarization antennas. With the phase of the two signals equal they are optimumly combined in a predetection combiner in a manner similar to that described by Brennan (1959). This combined signal is then used in conjunction with the common reference signal, to control a VCO which corrects for frequency changes in both horizontal and vertical signal channels. Consequently, under fading conditions, the probability that the primary loop will lose lock is less than the corresponding probability for the better of two signals alone. That is, when the signal in one channel fades to a level below that required to sustain lock, only this one channel loses lock. The primary loop and the other secondary loop remain locked. When the signal in this channel returns to a sufficient level, this secondary loop will automatically relock. Weighting voltages for the predetection combiner as well as automatic gain control voltages for the separate signal channel amplifiers are developed by coherent detection in the secondary loops.

The two input signals from the orthogonally polarized antenna are usually fluctuating in both phase and amplitude. Proper phase relationships for combining are obtained with the phase-lock loop system. The proper amplitudes for combining are obtained by the use of logarithmic attenuators actuated by the automatic gain control signals such that the channels are weighted according to their signal-to-noise ratios. The amplitude of the combined signal remains constant. This type of system has been very effective for polarization diversity reception of telemetry. It has been used extensively in the NASA Space Tracking and Data Acquisition Network.

Polarization diversity is also required for the autotrack functions of a data acquisition system. When a deep fade occurs, the receiving antenna is cross polarized to the incoming signal. The cross polarization pattern of an antenna is quite different from the in-polarization pattern. Consequently, the monopulse tracking null for cross polarization is shifted significantly from the antenna boresight axis. Typical examples of this are reported by Taylor (1967), and his record for the Tiros X satellite is reproduced in Figure 26. This Tiros X record was made with the STADAN 136-MHz telemetry antenna directed to point at the Tiros satellite. Two different monopulse autotrack receivers were connected to the antenna, one receiver on each of the two orthogonal linear polarizations. The sum channel automatic gain control (AGC) levels (which indicate received signal strength) and the X-axis and Y-axis tracking error signals were recorded as shown in Figure 26. Periods of significant polarization fading occurred for both the vertical and horizontal polarizations, but at different times during the

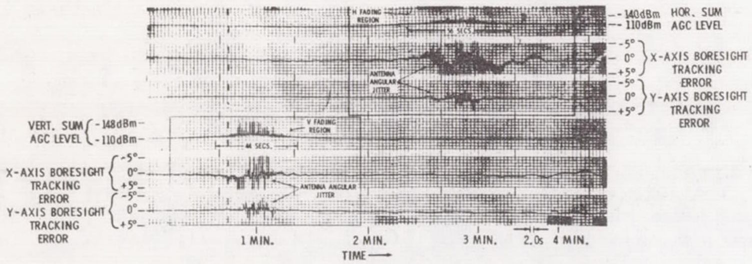

Figure 26. 136 MHz vertical and horizontal monopulse channel polarization fading characteristics for Tiros X satellite (Taylor, 1967).

satellite pass. This is to be expected because the very deep fades occur for almost complete cross polarization. The short-term signal fading is correlated with the satellite spin rate. The pattern of erroneous tracking error signals (indicated as antenna angular jitter) occurs in correlation with the deep nulls of the signal. If the monopulse tracking receivers had been connected to the antenna drive system, the erroneous tracking error signals would have driven the antenna away from the correct boresight position. The pattern on the record in Figure 26 shows a very large cyclical tracking error signal. Under operational conditions such a signal causes the antenna to go into wild oscillations. Polarization diversity monopulse receivers are the answer to this problem.

Taylor (1967) has developed an Automatic Polarization Diversity Autotrack Receiver (APDAR) for simultaneous-lobing monopulse systems. This APDAR receiver uses the multiple phase-lock loop technique described above that automatically tracks the phase of the two orthogonal polarization signals, compares phase to a coherent reference, and then provides coherent addition of the orthogonal polarization signals in a predetection diversity combiner. This phase-lock system maintains the phase-lock loop with the maximum signal under conditions of severe fades in one of the polarization channels. The phase-lock loop system in the two orthogonal sum channels are used to generate the referenced signals for the error channels. Error channels for both orthogonal polarizations are combined in a maximal-ratio diversity combiner in exactly the same manner as in the sum channel. The polarization diversity combiner eliminates the cross-polarized component in the vicinity of the null point by appropriate AGC weighting action.

Operational tests (Taylor, 1967) have demonstrated the excellent performance of the APDAR monopulse receiver under conditions of polarization fading. The

Goddard Range and Range Rate system for the new S-band frequencies will use the APDAR principle for autotrack.

The sum channel portion of the APDAR receiver has all of the polarization diversity characteristics needed for telemetry reception. Consequently, it is a very simple matter to provide receiver designs that perform both the monopulse autotrack function and the telemetry reception function simultaneously. This fits into the concept of unified tracking and data acquisition systems which make more effective use of the electronic systems through common equipment utilization. The new Goddard Range and Range Rate receiver will have the capability of simultaneous autotrack, ranging signal reception and telemetry reception. This follows the trend toward multi-function receivers. Multi-function receivers permit great operational flexibility at a multi-link ground station. Several identical receivers can be switched into or out of various telemetry links in order to provide each link with the required number of receiver channels. The required number of receivers changes from satellite to satellite. Hence, the stations need the capability to rapidly switch from one configuration to the other. Remote switching of many identical receivers provides this type of flexibility. Shaffer and King (1968) show that centralized control of these receivers aids the flexibility of operation and reduces the number of operating personnel required for the complex. The next generation of tracking and data acquisition receivers should have the capability of remote operation by either an operator or a digital computer.

C. Telemetry Data Handling

In the early days of space exploration, various types of telemetry systems were used on spacecraft. Gradually there has been a shift towards the use of pulse code modulation (PCM) telemetry for space exploration. The Apollo Unified S-Band system transmits analog voice and television and PCM telemetry from the spacecraft. PCM is the standard telemetry system for the NASA unmanned automated earth orbiting spacecraft. The reason for this trend is that PCM telemetry allows combining of all subchannels into one format and provides better transmission economy. Flexible and programmable PCM telemetry ground systems make possible demultiplexing and processing of PCM data received from a spacecraft in almost any format.

In PCM, the data is converted to digital form; the data from each channel is in the form of telemetry digital words. The words from each channel are time division multiplexed into a predetermined format. The format contains fixed length frames starting with frame synchronization words, format identification words, commutation sequence identification, and other identification words to enable the ground computers to properly handle the telemetry data. Frequency-shift keying or phase-shift keying are commonly used to modulate the telemetry carrier with the PCM bit train. Phase-shift keying is usually preferred because of the superior performance as illustrated in Figure 15.

In recent years significant progress has been made in the development of various coding systems for improving the telemetry system performance. The decoded data error rate is the measure of performance common to all telemetry systems. Figure 27 (Barnes, 1968) compares the performance of various coding systems used for telemetry. From these plots of group error probability versus signal-to-noise ratio (signal energy per information bit per noise power density), one can see the very large improvements in system performance that are possible through the use of coding systems. The two codes that provide the highest performance are convolutional codes. A convolutional code is an error detecting and correcting code in which sequential parity bits are mixed with the data bits. For example, a rate one-half convolutional code uses half of the bits transmitted for parity and the remaining half for data. An encoder for generating a rate one-half convolutional code is illustrated in Figure 28. The convolutional encoder is a binary shift register of length equal to the constraint length, K, of the code. Output taps of the shift register are connected to a modulo-2 adder for generation of parity. Initially the shift register is cleared to zeros. The first data bit is shifted into stage 1. The commutator sequentially samples the data bit in the first stage of the register and the parity output of the modulo-2 adder. The cycle repeats as each successive data bit is shifted into the register. This procedure continues until the last bit of the data block has been shifted into stage 1. Then the shift register is cleared to zero to start on the next block of data. In this example the generated code is alternately data and parity bits. Convolutional coding with sequential decoding has proven to be very powerful in improving the telemetry system performance as illustrated in Figure 27. Lumb's (50, 25) code is a rate one-half convolutional code with a 25 bit constraint length. This code system is to be used with the Pioneer spacecraft. The Barnes' (64, 32) code is also a rate one-half code which has a constraint length of 32 bits. It is planned for use on the Interplanetary Monitoring Platform (IMP) spacecraft. For a more detailed discussion of convolutional coding and sequential decoding, see Wozencraft and Jacobs (1965).

Most of the telemetry data for earth orbiting scientific spacecraft are recorded at the ground stations, and mailed back to a central processing facility. A minimum amount of data handling in real time is performed for control of the spacecraft. The control operations for many of the present-day spacecraft require conducting a series of command and telemetry operations which often cover the span of several ground stations. This type of operation makes it mandatory to have the central control of the spacecraft sequence at the central control center for the network. Generally each project has a control center from which it issues instructions to the network and receives telemetry data back from the network.

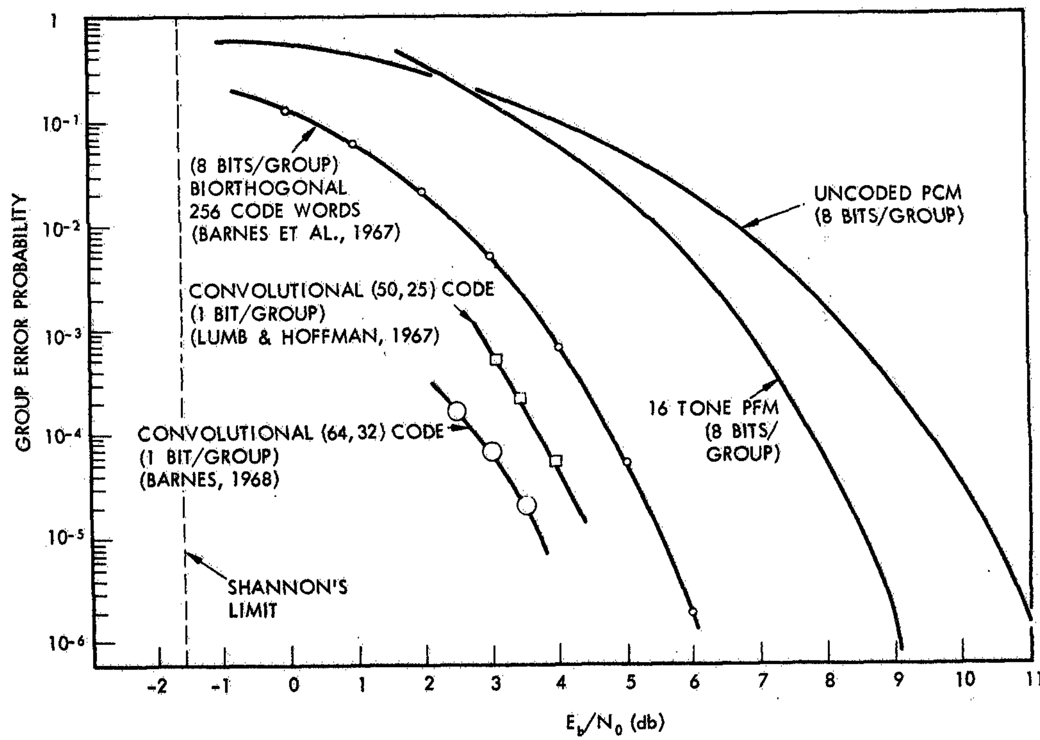

Figure 27. Comparison of telemetry system performance for uncoded PCM, 16 tone PFM, Biorthogonal code, and Convolutional codes (Barnes, 1968).

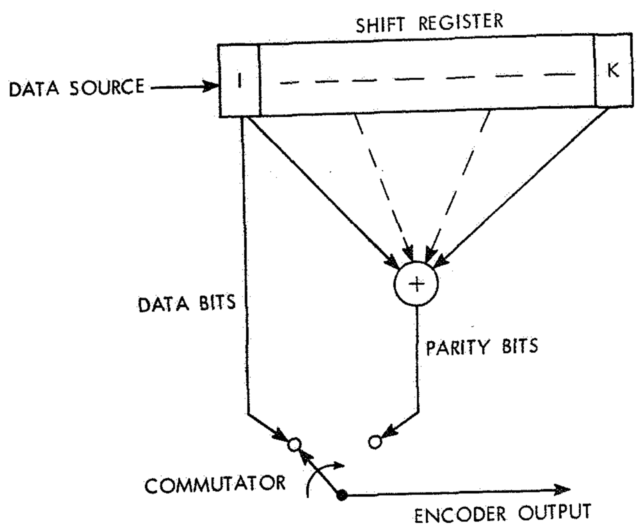

Figure 28. Block diagram of rate one-half convolutional encoder.

The use of PCM telemetry makes it possible to have extremely flexible data handling ground equipment at the stations which can handle many different satellite formats and transmit the data in digital form over commercial digital lines back to the central control center. For a real time transfer of data, the raw telemetry signals from the receiver is sent to a PCM signal conditioning unit which reconstructs the PCM data into a clean PCM bit stream. This digital data is then formatted and merged with time code and support data in the data transmission system input unit. The data is transmitted back to the control center via the NASA Communications Network (NASCOM). The NASCOM high-speed data communications system (Dickinson et al., 1966) is capable of operating at 600, 1200, and 2400 bits/second to most of the data acquisition stations.

In some instances the bit rate from the spacecraft exceeds the capability of the communications lines. Some operations only require certain selected telemetry channels to be sent back in real time. In that case the PCM data handling equipments have the capability of decommutating and selecting certain channels to be transferred to the data transmission system. In this way the needed data can be sent through the transmission lines.

In cases where the required data bit rate exceeds the communication line capability, computers are used to perform data compression operations. Data compression amounts to removing most of the redundancy in the data so that only the minimum number of bits are required to send the information over the data line. See Lynch (1967) for a more detailed discussion of data compression theory. Special computers for data compression are used at a few remote STADAN stations (where only 2400-bps circuits are available) for the Orbiting Astronomical Observatory.

For certain projects, such as the Nimbus weather satellite, the data transfer rate is far in excess of what can be handled over a 2400-bps communications line even if one were to use data compression. NASCOM has implemented microwave communications with the Fairbanks, Alaska and the Rosman, North Carolina stations for handling of the Nimbus weather data plus wideband data from several other spacecraft such as OAO.

D. Command Systems

At the central control center, the received real-time telemetry data is processed in a digital computer and displayed in the Project Operations Control Center. The project controller initiates instructions for the next operation with the satellite based upon the information from the telemetry read-out. At the present time, the instructions for command of the spacecraft are sent in one of three ways. The project controller may initiate a teletype message to the station with instructions to send a specific sequence of commands to the satellite. This is not a real time mode of command and is only sufficient under conditions when the station is being instructed for a command sequence on a satellite pass at a much later time. If near real time operations are required the project controller may instruct the station command operator directly by telephone. With the advent of the digital transmission systems, it has become practical to send commands reliably in real time directly from the Project Control Center to the station. The project controller sends a digital message over the data transmission system to the ground station. The digital command encoder system at the ground station receives the message and formats the command for transmission. The command may be sent to the spacecraft immediately or it may be delayed and transmitted at a precise time. The spacecraft receiving the command message decodes the command and performs the required action or places the message in storage for performance at a later prescribed time. The spacecraft receipt of the command message and the consequent action is telemetered back to the ground station and sent to the project controller in the central control facility. This closes the loop for real time control of many spacecraft operations.

In the early days of the space program the command activity was very limited and the capability for real-time command and control was not needed to any great extent. Consequently most of the early missions required the simplest command systems. Since then, however, there has been a steady trend toward more complex space functions, there has been a trend toward larger more sophisticated vehicles, and there has been a strong desire on the part of project personnel for more rapid response to operating needs. As a consequence, the requirements for extensive real-time control of satellite missions have been increasing, and at the present time the vast majority of the space missions require real-time control.

A wide range of command capability for NASA unmanned scientific spacecraft is provided in STADAN by the three standard command systems: the Address-Execute Tone command system, the Tone Digital command system, and the PCM Command Data system.

The Address-Execute Tone command system is intended for use where only a few 'on/off' type commands are required. In this system, the r.f. carrier of the ground command transmitter is amplitude modulated with a series of discrete single audio tones in the 1 to 7 kHz frequency range, as shown in Figure 29. Sequential transmission is employed with an address tone sent first to 'arm' the decoder. Each spacecraft is assigned a unique address tone. The execute tones follow to accomplish the particular command function and may consist of up to three tones in sequence. The execute tones may be any one of seven standard tones. The detection of these tones by the 'armed' spacecraft command decoder causes initiation of the command actions. After a preset period of time (equal to the length of the longest execute sequence) the decoder is automatically de-armed and cannot respond to an execute tone until it receives another valid address tone.

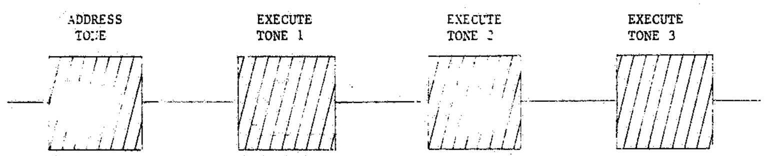

TONE DURATION:

0.5, 1.0, 1.5, 2.0, 2.5, 3.0, or 3.5 SECONDS

(DURATION CONSTANT THROUGHOUT SEQUENCE)

INTERVAL BETWEEN TONES:

0.5 SECONDS

Figure 29. Address-Execute Tone command structure.

Tone command systems employ relatively simple electronics in the decoder to achieve a high equipment reliability for retaining command control. This approach does not permit a 'secure' system and the probability of spurious commands from other radiating sources must be considered. Increased protection against spurious commands may be obtained by arming the decoder upon recognition of the trailing edge of the detected address tone rather than the leading edge. Since sequential transmission of tones is used, a decoder that prevents execution of a command if more than one tone indication at a time is detected during the sequence would offer increased protection. Protection against impulse interference may be achieved by selection of appropriate tone durations and incorporation of adequate integration times on the detected tone.

The Address-Execute Tone command system has been used successfully on many scientific spacecraft such as Alouette, Atmospheric Explorer B, Geodetic Satellite, Beacon Explorer, Interplanetary Monitor Platform, Radio Astronomy Explorer, UK International Satellite, and French VLF.

The Tone-Digital command system was developed for spacecraft requiring 70 or less, simple, real time, on/off commands. It basically consists of a 4 state (sync, 1, 0, blank) signal, pulse duration modulated (PDM), with constant bit ratio word coding and repetitive word formatting, as shown in Figure 30. A series of five words, each consisting of eight bits, 1 synchronization and 1 blank period are sent per command. The series consists of a unique address word sent twice followed by an execute word sent three times. The reception of one correct address word and one valid execute word in the same series of five words is sufficient to effect a command. This redundancy increases the probability of receiving the correct command under weak signal and interference conditions.

The technique used for error detection and interference rejection consists of forming the code words from a fixed number of zeros and ones. The address code consists of a combination of two ones and six zeros. The execute code always contains a combination of four ones and four zeros. This 4 × 4 code provides 70 commands out of the possible 256 binary combinations of the eight data bits. This fixed 4-out-of-8 bit coding provides a means of detecting all odd and 43% of all two bit errors. To further lessen the possibility of spurious commanding, no address or execute word may be decoded unless a sync pulse is detected, and once the address has been detected, a valid execute word must be read within a fixed period.

Pulse duration modulation of an audio subcarrier is used for the bit coding. A bit period is 72 cycles of the subcarrier frequency. The sync bit is 54 cycles, the '1' bit is 36 cycles, and the '0' bit is 18 cycles of the subcarrier frequency.

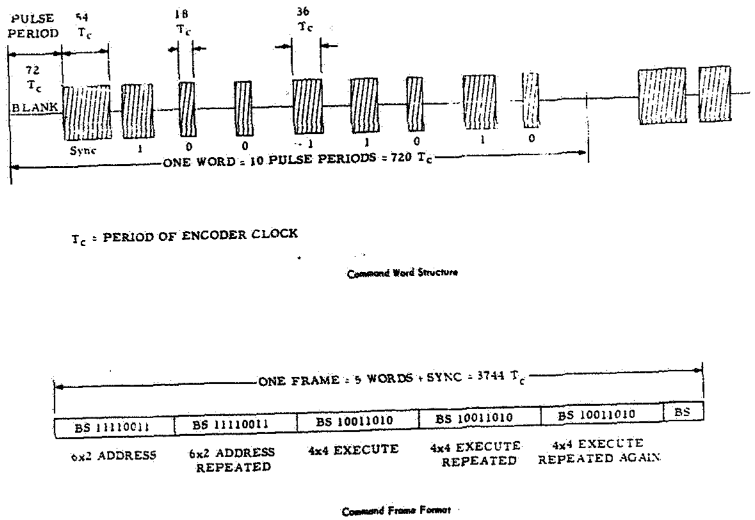

Figure 30. Tone-Digital command word structure and format.

The subcarrier frequency amplitude modulates the transmitter carrier to produce a PDM/AM/AM mode. These subcarrier frequencies are assigned one tone per spacecraft. They are in the 7- to 11-kHz band.

This system has been used by a number of spacecraft including the Orbiting Solar Observatory (OSO), Pegasus, Bios, INJUN, HEOS, and ESRO.

The NASA PCM Command Data system is a high capacity binary up-data link for transmitting commands to spacecrafts. The command message configuration is similar to a computer instruction, as partitioning is used to designate various functions, such as addressing, event timing, error checking, subsystem control, etc.

The command signal can be categorized as PCM/FSK-AM/AM. The initial bit modulation is PCM-NRZ. The pulse code is frequency modulated into an intermediate passband by coherently switching a subcarrier oscillator between two assigned frequencies in the 7 to 12 kHz band. A sinusoidal bit synchronization signal (bit rate timing) is 50% amplitude modulated onto these data subcarriers. The composite audio waveform is shown in Figure 31. Final peak r.f. carrier modulation is nominally 80% AM.

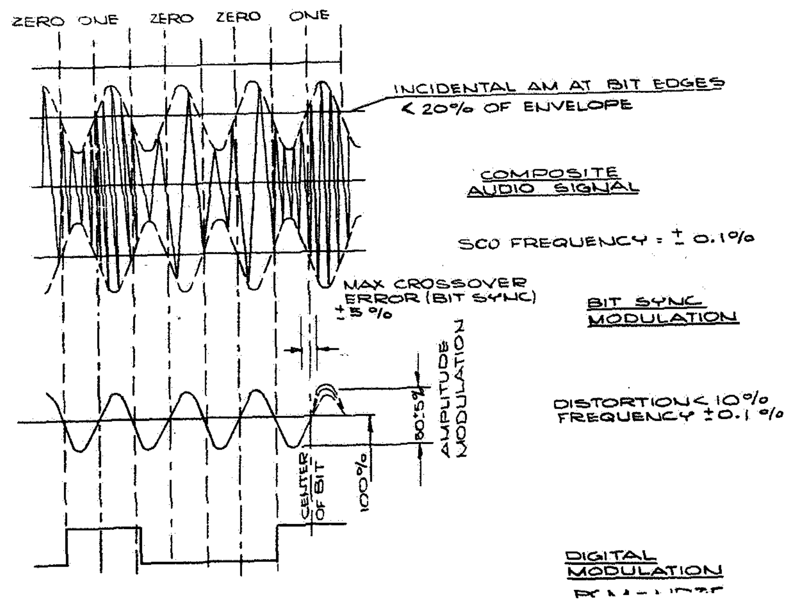

Figure 31. PCM command composite audio waveform.

The hierarchy of command data is the bit, frame and message in that order. The frame is the minimum group of bits that make up a single command transmission. As a typical example, a frame might contain a spacecraft address followed by a command, a command complement, a memory load instruction, or a time tag. The frame is divided into a noninterrupted group of bits. For any one spacecraft the number of bits in each of the frames is the same for all commands. Two message formats are available, the command format and the memory load format (see Figure 32). In the command format the maximum frame length is 64 bits and any number of frames can be transmitted until end of message. Each frame contains a spacecraft address which is different for each spacecraft. The address activates the spacecraft decoder for a period of time sufficient to receive the command message. In memory load format, a standard frame is followed by a number of bits, not to exceed 4096 bits. This number of bits is an integral multiple of the number of bits assigned to the frame. Not

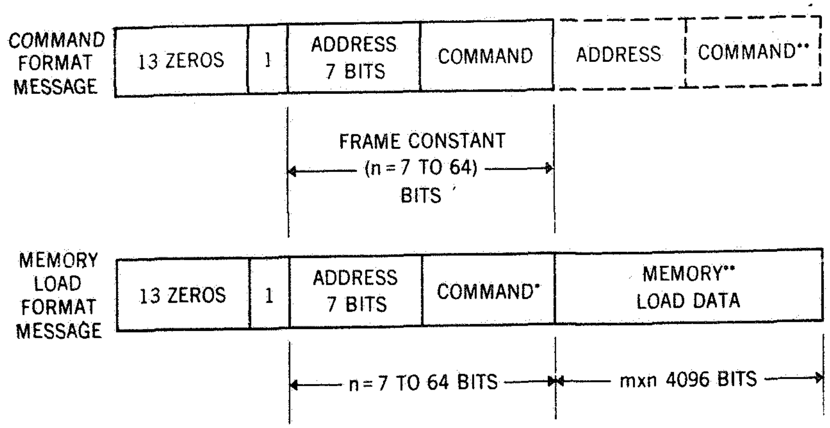

n IS ASSIGNED ONE VALUE FOR ANY ONE SPACECRAFT.

m IS AN INTEGER AND ASSIGNED NOT MORE THAN FOUR VALUES FOR ANY ONE SPACECRAFT.

* MEMORY LOAD INSTRUCTION COMMAND.
MUST BE A HAMMING DISTANCE OF AT LEAST 2 FROM ANY OTHER COMMAND

** THERE WILL BE A BREAK OF SUBCARRIER BETWEEN MESSAGES.

Figure 32. Command format and memory load format of the PCM Command Data System.

more than four different multiples may be used by any one spacecraft. A message is preceded by a minimum of 13 'zeros' and a 'one' for synchronization purposes. A break of subcarrier occurs after every message.

Transmission of PCM command data from the GSFC Operations Control Centers to the remote STADAN command sites is via the NASCOM High-Speed Data (digital) Transmission System or the NASCOM Teletype System. The FSK subcarriers are generated at the remote STADAN command sites.

A word might be said at this point on command verification. All command and control data transmitted to a spacecraft is checked at the ground station and in the spacecraft for bit errors prior to execution or storage. At the ground station, each bit transmitted is detected in a monitoring receiver and is looped back to the command encoder where it is compared with the intended bit in the output of the command register. If the comparison is false, the command encoder enters an error mode with provisions to stop or repeat the command.

There are a number of ways to verify the receipt of a correct command in the spacecraft. Some projects send part or all of the command frame twice, first true then complement, and these are compared in the spacecraft command decoder. Another method is to encode each command with an error detection code or parity bits which are checked in the spacecraft decoder. The result of the error check is telemetered to the transmitting ground station.

The most advanced system for command and control of a manned spacecraft is the Apollo Unified S-Band System. The Apollo mission is more complex than either the Mercury or Gemini programs. Consequently, the system for command and control of Apollo (Knox, 1965) has a greater capability. As described earlier, the Unified S-Band system uses a single carrier frequency for the uplink transmission of tracking signals, command data, and voice to the spacecraft.

Commands for the Apollo spacecraft are generated in the Mission Control Center (Houston, Texas), transmitted via data circuits to the remote ground station, validated and stored in the command data processor. At a selected time, a flight controller, either at MCC or at the ground station, sends an execute instruction to the command data processor and the command is sent to the spacecraft. Also, in some cases, the command from the Mission Control Center is validated at the ground station and immediately transmitted to the spacecraft.

The Apollo commands may be classified as real time 'on/off' type commands, computer load commands, and timing data commands. The command word structure consists of four different word lengths with similar formats as shown in Figure 33. The four available word lengths are 12 bits, 22 bits, 30 bits, and 35 bits. The first seven bits are used for vehicle address and on-board system address. The remaining bits are for instructions and control. Each bit consists of five sub-bits. This is done for added security and to provide for rejection of non-valid commands. Additional protection is gained by encoding the vehicle address sub-bits with a different code than the remainder of the data sub-bits. The system address sub-bits and the data sub-bits coding is the same. The sub-bits code for a 'zero' is the complement of the sub-bit code for a 'one'. Since all command messages will be generated at the Mission Control Center, additional control bits are added to the message to insure that the commands are transmitted safely to the remote site and from the remote site to the spacecraft. These control bits are redundant complementary bits, symbol repeat bits and parity bits.

The data sub-bits are transmitted to the spacecraft at a 1-kHz rate. Each sub-bit controls a 2-kHz phase shift keyed (PSK) oscillator that is shifted 180° by a change of state from a 'one' or a 'zero'. The output of the 2-kHz oscillator is added with a coherent 1-kHz signal that is transmitted for synchronization

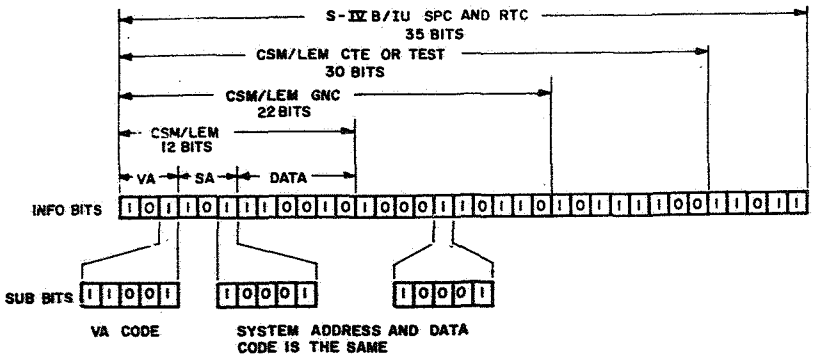

Figure 33. Apollo/Saturn command word structure.

purposes. A 'one' is defined as a composite signal where the 1-kHz and 2-kHz signals are going positive at the zero cross-over point.

Ground verification of transmission of a correct command is obtained with receivers which detect the transmitted data and return it to the computer for validation.

When the spacecraft receives a command message it performs several checks to determine if the command is valid. A command will be accepted by the spacecraft only if it has the correct vehicle address, systems address, bit structure, and word length. A message acceptance pulse (MAP) is telemetered from the spacecraft to the ground station when a valid command is received. If a MAP is not received, the command word is retransmitted a preselected number of times. Continued failure to receive a MAP alerts the flight controller. A printout that includes up-data transmission, the time of transmission, and an indication that the command was or was not received is available as command history.

5. NEXT GENERATION TRACKING AND DATA ACQUISITION NETWORKS

All of the present day tracking and data acquisition networks have a basic deficiency in that they cannot provide 100% contact with a spacecraft in a low earth orbit. For example, the total Manned Space Flight Network contact time with a spacecraft in a 200- to 500-km circular orbit is in the order of only 10 to 20%. For a manned mission this means that there is a large percentage of

the time when it is impossible to communicate with the astronauts in orbit. For unmanned spacecraft this means that the operation of the spacecraft must be programmed through the periods of no station contact, and the data must be stored in the spacecraft for later relay at the time of contact with a ground station. The majority of the spacecraft use tape recorders for storing the data for later playback. The average useful life of a spacecraft in orbit today is approximately 2 years. However the average lifetime of a spacecraft tape recorder is only 3 months. Thus on the average a spacecraft must operate without a recorder for approximately 3/4 of its useful lifetime. In addition to reliability, there is a problem due to the finite limit of the onboard storage system capacity. If the mission requirements for data storage exceed the capacity of existing storage mediums, then some other way must be found to return the data to the user on the ground. If it were possible to have 100% contact time between the ground and the spacecraft, then this wide-band data could be transmitted in real time, thus avoiding the storage problem.

It was mentioned earlier in this paper that earth orbiting spacecraft need to be tracked at only a few points in each orbit in order to determine the spacecraft orbit and position to a sufficient accuracy for the mission requirements. This is true only for the unperturbed orbits for which the computation can extend over three or more orbits. In cases where there are thrusting maneuvers which change the orbit, tracking is usually required throughout the thrusting period and for some short period afterward to enable the transition to be determined with precision. The manned missions have a number of such critical maneuvers and they utilize mobile tracking ships and aircraft for obtaining critical coverage of powered phases of the mission.

There has been a considerable amount of study of the question how best to provide 100% coverage of low earth-orbiting missions. One of the more attractive solutions is a network of synchronous-orbit Tracking and Data Relay Satellites. In this system the low-orbiting spacecraft would establish its tracking and data acquisition link to the ground station via the synchronous relay satellite. The ground station would transmit command and tracking signals up to the synchronous relay satellite, which in turn relays the signal to the low-orbiting spacecraft. The telemetry and return tracking signals from the low-orbiting spacecraft are transmitted to the synchronous relay satellite, which relays them down to the ground station. Three Tracking and Data Relay Satellites equally spaced around the circumference of the earth would provide 100% contact time with any low-orbiting spacecraft. The tracking of powered flight phases of space missions would require simultaneous tracking by at least two Tracking and Data Relay Satellites in order to get the necessary geometry for rapid position and velocity determination. A configuration of four Tracking and Data Relay Satellites, as shown in Figure 34, provides the simultaneous tracking capability by at

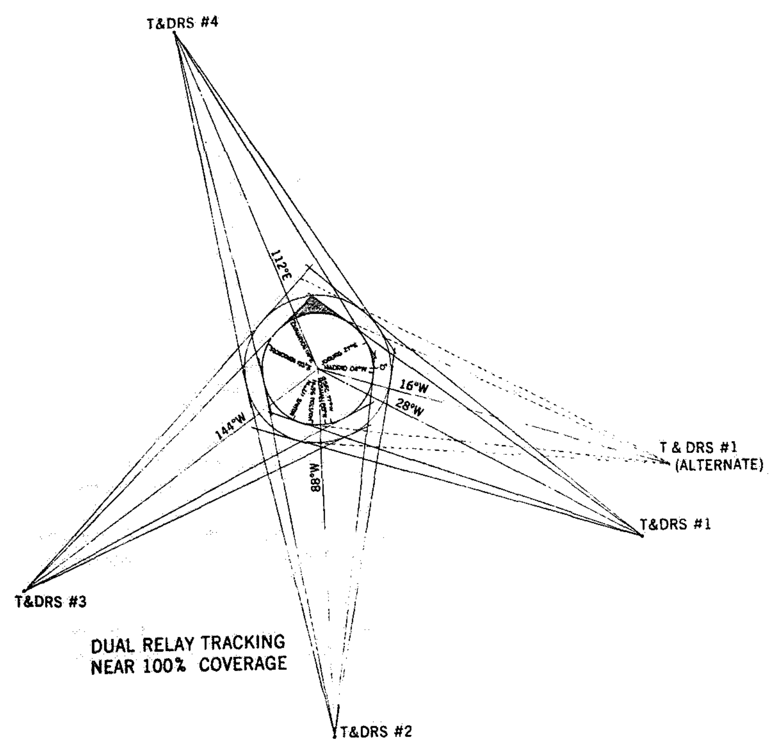

Figure 34. Orbit Configuration for a synchronous orbit Tracking and Data Relay Satellite network.

least two Tracking and Data Relay Satellites. In addition the four satellites configuration provides in-orbit redundancy for data acquisition. One of the spacecraft could fail and the remaining three would still provide telemetry coverage. The Tracking and Data Relay Satellites 1, 2, and 3 are located such that they can be viewed by the same ground station. The Tracking and Data Relay Satellite number 4 is not in view of the ground station, but it appears feasible to perform a double relay via Tracking and Data Relay Satellites number 3 or number 1. In this manner only one ground station complex would be required for the entire network of Tracking and Data Relay Satellites.

In concept the Tracking and Data Relay Satellite network is very simple, but in a technical sense it is extremely complicated. There are many satellites in low earth orbits and consequently a Tracking and Data Relay Satellite network must have the capability to work simultaneously with a large number of user spacecraft. Thus the relay function must be performed in multiple channels. The antenna gain on the Tracking and Data Relay Satellite must be fairly high in order to perform the network function effectively because the range from a synchronous-orbit spacecraft to a low-orbit user spacecraft will be much greater than the usual range between a ground station and the low-orbit spacecraft. This increase in range must be compensated for by either increased antenna gain or by increased radiated power. The system becomes very attractive for stabilized low-earth orbiting spacecraft which can utilize a directive antenna for sending telemetry and tracking to a Tracking and Data Relay Satellite. User spacecraft with omnidirectional antennas require a high antenna gain on the Tracking and Data Relay Satellite or higher transmitter power. A high-gain antenna has a narrow beamwidth. If the beamwidth is narrower than 24°, then the beam of the Tracking and Data Relay Satellite antenna must be steered to follow the low-orbiting spacecraft. Systems calculations have shown that for frequencies above the VHF band the antenna beamwidths will be smaller than 24° and hence must have beam steering capability.

The choice of frequencies to use for the Tracking and Data Relay Satellite operation invoice a number of different considerations. If the user spacecraft has an omnidirectional antenna, the power received at the Tracking and Data Relay Satellite is a function only of the transmitted power, the range and the Tracking and Data Relay Satellite antenna area. It is independent of frequency. Since the beamwidth of an antenna increases with decreasing frequency, it would be advantageous to operate at very low frequencies for communicating with an omnidirectional satellite in order to avoid the necessity of beam steering. In contrast, when the user spacecraft is stabilized such that it could use a fixed-area directed antenna, the received power is proportional to the transmitted power, the area of the user satellite antenna, the area of the Tracking and Data Relay Satellite antenna, the reciprocal of the range squared, and the frequency squared. Thus the higher the frequency, the better is the system performance.

These two cases appear to lead to opposite frequency requirements. However, other technical considerations come into consideration and indicate the necessity of certain compromises. When an omnidirectional antenna is used on a low-orbiting spacecraft, multipath propagation is to be expected because of the reflection of the signals from the earth. The severity of the multipath under these conditions at VHF has not been fully evaluated as yet. Directive antennas on the user spacecraft would greatly reduce the multipath. Thus if multipath turns out to be a serious problem, it may be necessary for all user spacecraft to provide antenna directivity which would reduce the multipath. Other schemes of combating multipath, such as coding techniques, are also under investigation. The problems on the high end of the frequency extreme are that solid state transmitter and receiver technology has not progressed sufficiently far to be able to make highly efficient and reliable repeater systems at frequencies significantly higher than a few thousand megahertz. Another problem is that if frequencies are very high, the antenna beamwidths become extremely narrow and acquisition becomes much more difficult.

These considerations lead to the conclusion that with the present day spacecraft technology a frequency of about 2000 MHz is reasonable to use between a user spacecraft and a synchronous-orbit Tracking and Data Relay Satellite. Orbital tests of some of the Tracking and Data Relay Satellite system concepts are being planned as part of the NASA Advanced Technology Satellite program. The ATS-F spacecraft will have a 30-foot diameter parabolic antenna. It will have the capability both mechanically and electronically to steer the beam of the parabola, and it will have a transponder for relay of ground-transmitted signals to a user spacecraft and vice versa. It is planned to conduct a data relay and tracking experiment to track and acquire data from the Nimbus spacecraft via the ATS-F spacecraft. In addition, a laser communications experiment is planned for ATS-F which would develop the technology for use of laser frequencies (10.6 microns) for wide-band tracking and data relay between two Tracking and Data Relay Satellites.

The advancing space technology should make a synchronous-orbit Tracking and Data Relay Satellite system feasible in the near future. Such a system has the potential of providing full orbit tracking, real-time data acquisition, faster and more efficient data processing, real-time command capability, elimination of spacecraft bulk data storage, 100% mission voice coverage for manned flight missions, and a much greater capability for wide-band data gathering. Interestingly enough, the economic considerations appear to be in favor of such an orbiting network. Preliminary cost studies have indicated that the potential exists for eliminating enough of the tracking ships, aircraft, and remote ground stations to realize a cost savings in excess of the cost for placing the synchronous satellites in orbit. Many of the existing ground stations would have to be retained in the network in order to support the spacecraft that have orbits higher than about 5000 km. However the net result would be a reduction in the number of ground stations for providing the necessary support. A tracking and data acquisition network consisting of synchronous orbit Tracking and Data Relay Satellites plus a minimum number of ground stations is a very attractive candidate to be the next generation tracking and data acquisition network.

REFERENCES

Alley, C. O., Bender, P. L., Dicke, R. H., Faller, J. E., Franken, P. A., Plotkin, H. H., and Wilkinson, D. T.: 1965, 'Optical Radar Using a Corner Reflector on the Moon', J. Geophys. Res. 70, 2267-9.

Baghdady, E. J. and Kruse, K. W.: 1964, 'The Design of Signals for Space Communications and Tracking', 1964, IEEE International Convention Record, Part 7, 152-174.

Balakrishnan, A. V. (ed.): 1963, Space Communications, McGraw Hill, New York.

Barnes, W. P.: 1968, 'A Simulation of Convolutional Encoding with Sequential Decoding with Application to IMP-I and AIMP-H, J. Data Processing', Goddard Space Flight Center Rept. X-563-68-65.

Baumert, L., Easterling, M., Golomb, S. W., and Viterbi, A.: 1961, 'Coding Theory and Its Applications to Communications Systems', Jet Propulsion Lab. Tech. Rept. No. 32-67 (NASw-6).

Benoit, A.: 1968, 'Signal Attenuation Due to Neutral Oxygen and Water Vapour, Rain and Clouds', Microwave J. 11, No. 11, 73-80.

Bivas, R., Morael-Courtois, N.: 1966, 'Determination de l'orbite du satellite GEOS-A au moyen d'un télémetre à laser a partir d'une station' Comp. Rend. 262, 935.

Brennan, D. G.: 1959, 'Linear Diversity Combining Techniques', Proc. IRE 47, 1075-1102.

Bunce, R. C.: 1965, 'Receiver Exciter Subsystem', Proc. Apollo USB Tech. Conf., NASA SP-87, 59-73.

Coates, R. J.: 1960, 'Worldwide Tracking, Timing, and Data Processing Facilities', Proc. 6th National Flight Test Instr. Symp., Instr. Soc. Amer.

Coates, R. J. and Golden, T. S.: 1968, 'Ionospheric Effects on Telemetry and Tracking Signals from Orbiting Spacecraft', IEEE National Telemetering Conf. Record, IEEE No. 68-C-8-NTC, 43-48.

Cohen, W. and Steinmetz, C. M.: 1959, 'Amplitude and Phase-Sensing Monopulse System Parameters', Microwave J. 2, 27-33 and 33-38.

Dicke, R. H.: 1946, 'The Measurement of Thermal Radiation at Microwave Frequencies', Rev. Sci. Instrum. 17, 268.

Dickinson, W. B., Wilson, D. D. and Turner, V. E.: 1966, 'Implementation of a Worldwide High-Speed Data-Transmission System for NASA Mission Support', Goddard Space Flight Center Report X-500-66-402.

DiLosa, V. J.: 1966, 'Diversity-Lock Phase Demodulator', NASA Tech. Note TN D-3342.

ESSA Environmental Data Service: 1966, 1967, 'Solar-Geophysical Data', Institute for Environmental Research Reports FB-259 through 278.

Filipowski, R. F. and Muhldorf, E. I.: 1965, Space Communications Systems, Prentice-Hall, New Jersey.

Fitzgerald, P. T., Engels, P. D., Shaffer, H. W., Habib, E. J., and Mitchko, M. J., 1964, 'A Hybrid Ranging System for Spacecraft', NASA Goddard Space Flight Center Report X-531-64-71.

Fremouw, E. J.: 1966, 'Radiowave Scattering Structure in the Disturbed Auroral Ionosphere: Some Measured Properties', Geophysical Institute of U. of Alaska Rept. UAR R-180, vols. I and II.

Gabriel, W. F.: 1966, 'Preliminary Antenna Design Considerations for a STADAN Relay Satellite System', Goddard Space Flight Center Rept. X-520-66-107.

Goddard Space Flight Center: 1964, 'Satellite Tracking and Data Acquisition Network Facilities Report', Goddard Space Flight Center Rept. X-539-64-159.

Golden, T.: 1968, 'A Proposal for Measuring the Correlation Distance of Equatorial Ionospheric Disturbances', Goddard Space Flight Center Rept. X-525-68-302.

Habib, E. J., Kronmiller, G. C., Engels, P. D. and Franks, H. J.: 1964, 'Development of a Range and Range Rate Spacecraft Tracking System', NASA Tech. Note TND-2093.

Hocking, W.: 1965, 'Shipboard Doppler Counter, Antenna Programmer and Tracking Data Processor', Proc. Apollo USB Tech. Conf., NASA SP-87, 109-124.

Hogg, D. C.: 1959, 'Effective Antenna Temperatures Due to Oxygen and Water Vapor in the Atmosphere', J. Appl. Phys. 30, 1417.

Hogg, D. C.: 1968, 'Millimeter-Wave Communications Through the Atmosphere', Science 159, 39-46.

Holzman, R. E.: 1968, 'Tracking Data System', Jet Propulsion Lab., S.P.S. 37-51, vol. II, pp. 3-10.

Hood, B.: 1965, 'Command and Service Module Unified S-Band System', Apollo USB Tech. Conf., NASA SP-87, 223-232.

Horner, F.: 1960, 'Extraterrestrial Radio Noise as a Source of Interference in the Range 30-1000 Mcs', Proc. Inst. Elect. Eng. Part B 107, 373-376.

Iliff, R. L.: 1965, 'Photographing Satellite-Reflected Laser Pulses for Geodetic Stereo Triangulation', J. Geophys. Res. 70, 3505.

Jet Propulsion Laboratory: 1963, 'Mark I Ranging Subsystem', JPL S.P.S. 37-20, vol. III, pp. 12-15.

Jet Propulsion Laboratory: 1964, 'Mark I Ranging Subsystem-Code Components Acquisition and Code Correlation', JPL S.P.S. 37-29, vol. III, pp. 12-19.

Johnson, T. S., Plotkin, H. H., and Spadin, P. L.: 1967, 'A Laser Satellite Ranging System-Part I: Equipment Description', IEEE J. Quantum Electr. QE-3, 435-439.

Kelleher, J. J. and Binkley, W. O.: 1968, 'Millimeter Wavelengths for Space Communications', Microwave J. 11, 30-36.

Kent, G. S. and Koster, J. R.: 1966, 'Some Studies of Night-Time F Layer Irregularities at the Equator Using VHF Signals Radiated from Earth Satellites', Spread F and Its Effects Upon Radiowave Propagation (ed. by Newman, P.) W. & J. MacKay Co., London, pp. 333-356.

Knox, C. B.: 1965, 'Apollo Digital Command System', Proc. Apollo USB Tech. Conf., NASA SP-87, 191-203.

Ko, H. C.: 1958, 'The Distribution of Cosmic Radio Background Radiation', Proc. IRE 46, 208.

Krassner, G. N.: 1964, Introduction to Space Communication Systems, McGraw-Hill, New York.

Kronmiller, G. C. and Baghdady, E. J.: 1965, 'The Goddard Range and Range Rate Tracking System: Concept, Design, and Performance', NASA Goddard Space Flight Center Rept. X-531-65-403.

Kronmiller, G. C. and Zillig, D. J.: 1967, 'The Goddard Range Rate System Performance While Tracking IMP-F', NASA Goddard Space Flight Center Rept. X-571-67-532.

Kuykendall, W.: 1965, 'Lunar Excursion Module Unified S-Band System', Apollo USB Tech. Conf., NASA SP-87, 233-242.

Lantz, P. A. and Thibodeau, G. R.: 1967, 'NASA Space-Directed Antennas', Goddard Space Flight Center Rept. X-525-67-430.

Laughlin, C. R.: 1963, 'The Diversity-Locked Loop - A Coherent Combiner', IEEE Trans. on Space Electr. and Telem. SET-9, 84-92.

Lawton, J. G.: 1958, 'Comparison of Binary Data Systems', Proc. Second National Convention of Military Electronics, IRE, p. 54.

Lehr, C. G., Maestra, L. A., and Anderson, P. H.: 1967, Space Research, vol. VII, North Holland Pub. Co., Amsterdam, p. 723.

Lindley, P.: 1965, 'Ranging Subsystem - Mark I', Proc. Apollo USB Tech. Conf., NASA SP-87, 99-107.

Lockheed Missiles & Space Co.: 1967, 'Orbiting Data Relay Network Study', Final Report Contract NASW-1446.

Lumb, D. R.: 1967, 'A Study of Codes for Deep Space Telemetry', Proc. IEEE International Convention.

Lumb, D. R. and Hofman, L. B.: 1967, 'An Efficient Coding System for Deep Space Probes with Specific Application to Pioneer Missions', NASA Tech. Note. TN D-4105.

Lynch, T. J.: 1967, 'Data Compression with Error-Control Coding for Space Telemetry', NASA Tech. Rept., NASA TR R-261.

Marsh, J. G., Doll, C. E., Sandifer, R. J., and Taylor, W. A.: 1967, 'Intercomparison of the Minitrack and Optical Tracking Networks using GEOS-I Long Arc Orbital Solutions', Goddard Space Flight Center Rept. X-552-68-105.

Medhurst, R. G.: 1965, 'Rainfall Attenuation of Centimeter Waves: Comparison of Theory and Measurement', IEEE Trans. Ant. and Propag. AP-13, 550-564.

Mengel, J. T. and Herget, P.: 1958, 'Tracking Satellites by Radio', Sci. Amer. 198, 23-29.

Moorehead, R. W. and Arndt, G. D.: 1968, 'The Apollo Unified S-Band Telecommunications System', IEEE Nat. Telemetering Conf. Rec., IEEE Cat. No. 68-C-8-NTC, 251-261.

Moss, S. J. and Wells, W. T.: 1967, 'A Laser Satellite Ranging System-Part II: An Analysis of the GSFC Laser Ranging Data', IEEE J. Quantum Electr., QE-3, 440-445.

Painter, J. H.: 1367, 'Designing Pseudorandom Coded Ranging Systems', IEEE Trans. Aerospace Electr. Syst., AES-3, 14-27.

Plotkin, H. H.: 1964, 'The S-66 Laser Satellite Tracking Experiment', Quantum Electronics III, vol. II, Columbia Univ. Press, New York, p. 1319.

Plotkin, H. H., Johnson, T. S., Spadin, P. and Moye, J.: 1965, 'Reflection of Ruby Laser Radiation from Explorer XXII', Proc. IEEE 53, 301-2.

Potter, P. D.: 1963, 'A New Horn Antenna with Suppressed Sidelobes and Equal Beamwidths', Microwave J. 6, 71-78.

Radio Corporation of America: 1967, 'Orbiting Data Relay Network', Final Report Contract NASW-1447, AED R-3152.

Rhodes, D. R.: 1959, Introduction to Monopulse, McGraw-Hill, New York.

Rolinski, A. J., Carlson, D. J., and Coates, R. J.: 1962, 'The X-Y Antenna Mount for Data Acquisition from Satellites', IRE Trans. Prof. Group Space Electr. and Telemetry, SET-8, 159-163.

Schmid, P. E.: 1967, 'The Feasibility of a Direct Relay of Apollo Spacecraft Data Via A Communications Satellite', NASA Tech. Note, NASA TN D-4048.

Schroeder, C. A.: 1960, 'Electronic Interferometer Tracking', Fifth Nat. Symp. on Space Electronics and Telemetry, IRE Trans. PGSET, 9.4.

Schwartz, M., Bennett, W. R. and Stein, S.: 1966, Communications Systems and Techniques, McGraw-Hill, New York.

Shaffer, H. W. and King, E. L.: 1968, 'Multifunction Receiver for Integrated Tracking, Telemetry and Ranging Data Acquisition', Proc. International Telemetry Conf. 4, 134-148.

Shannon, C. E. and Weaver, W.: 1949, The Mathematical Theory of Communications, University of Illinois Press, Urbana.

Snyder, G. L., Hurst, S. R., Grafinger, A. B., and Halsey, H. W.: 1965, 'Satellite Laser Ranging Equipment', Proc. IEEE 53, 298.

Taylor, R. E.: 1967, 'Satellite Tracking Simultaneous-Lobing Monopulse Receiving System with Polarization Diversity Capability', IEEE Trans. Aerospace Electr. Syst. AES-3, 664-680.

Tsao, C. K. H., deBettencourt, J. T., and Kullstam, P. A.: 1968, 'Design of Millimeter Wave Communication Systems', Microwave J. 11, 47-51.

Varson, W. P.: 1965, 'Functional Description of Unified S-Band System and Integration into the Manned Space Flight Network', Proc. Apollo USB Tech. Conf., NASA SP-87, 3-12.

Vonbun, F. O. and Mengel, J. T.: 1968, 'Tracking and Communications for Planetary Manned Missions', J. Spacecraft Rockets 5, 863-865.

Wozencraft, J. M. and Reiffen, B.: 1961, Sequential Decoding, John Wiley & Sons, New York.

Wozencraft, J. M. and Jacobs, I. M.: 1965, Principles of Communication Engineering, John Wiley & Sons, New York.

Zonge, K. L. and Fremouw, E. J.: 1967, 'Aberrations of Radio Signals Traversing the Auroral Ionosphere', Geophysical Inst. of Univ. of Alaska, NASA Contract NAS5-3940 Annual Report.